NMR Study on Ion-Molecule Interaction

by

Koichi Miura

1986

CONTENTS

Chapter I

Introduction

In solution molecules and ions are distributed to retain a certain degree of a regular structure and arrangement, while they microscopically undergo translational, rotational, and vibrational motions. Microscopic and macroscopic characters of solution depend on the structure and property of individual molecules and ions. Furthermore, macroscopic characters closely relate to the microscopic characters through the structure and property of molecular clusters. Up to the present, various kinds of techniques have been applied to investigate solution structures. Infrared and Raman spectroscopic techniques are used for the investigation of hydrogen bonding in solution with measuring the shift in vibrational and rotational frequencies.[1] NMR (nuclear magnetic resonance) technique is applied to the investigation of solute-solvent interaction[2] and of dynamical rotational and translational motions of liquid molecules.[3] Dielectric constant measurement is also made use of the study of molecular orientation.[4] X-ray diffraction and neutron diffraction methods give information for complex formation and molecular configurations in liquid states.[5]

The author have performed a physicochemical study on

simple electrolytes in solutions by the use of FT(Fourier transform)-NMR apparatus. A great number of works applying the NMR technique to electrolytic solutions have been reported by many investigators, and a lot of reviews were published.[6-15] However, the greater part of those works belong to the NMR studies on paramagnetic salt solutions, and the works on diamagnetic electrolytes are rather scarce. Therefore, I made an NMR study on the diamagnetic ion-molecule (water and trihalomethanes) interactions. Especially I concentrated on the diamagnetic ion-water complexations in acetone solvent. Water solvent is inappropriate to observe the ion-water associations because water solutions have a too complicated hydrogen bonding network. An inert solvent such as acetone is appropriate as a solvent to examine an ion-water association reaction.

It is desirable to get both static and dynamic information on the ion-molecule interactions. The author measured ^{1}H chemical shifts, ^{35}Cl absorption line widths, and ^{1}H spin-lattice relaxation times in diamagnetic salt solutions, and he analyzed them to get the static and dynamic information on the ion-molecule complexations. Furthermore, a quantum mechanical calculation for the chemical shift changes due to ion-water associations was performed in order to compare the theoretically estimated

complex formation shifts with the experimentally determined shifts. These works are reported separately in this thesis.

Chapter II of this thesis is a presentation and an analysis of the proton NMR chemical shift data for the ion -water interactions in acetone solvent.[16] The measured water proton chemical shifts for the complex formation reactions with diamagnetic ions are analyzed to get the complex formation shifts and the equilibrium constants of association. The physicochemical parameters having an effect on the complex shift and the association constant are discussed.

In Chapter III, the author presents the calculated results for the complex formation shifts. Theoretical calculations for the nuclear shielding constants of water hydrogen and oxygen atoms are performed on the basis of the point charge model.[17] The theoretical complex formation shift is evaluated as a difference between the shielding constants without and with a point charge, and is compared with the experimental shift obtained in Chapter II.

In Chapter IV, the author states the measurements of the proton chemical shift and the ^{35}Cl line width of a weakly hydrogen bonded complex between a Cl^- ion and a trihalomethane molecule ($CHCl_3$ or $CHBr_3$) in some solvents.[18] Using the same analysis as that in Chapter II, the complexed

line widths of Cl^- ion, the complex proton shifts of trihalomethanes, and the association constants are evaluated. The solvent dependence of these parameters are investigated.

Finally, in Chapter V, the author mentions the measurements of the water proton spin-lattice relaxation times, T_1, performed to get an information on the dynamical motion of water molecule bound to Al^{3+} ion.[19] When the aqueous solutions including Al^{3+} ions are cooled, the exchange between the free and bound water molecules is slowed and the water signals separates into each component of the free and bound waters. Analyzing the measured T_1 values, information on rotational motions of the coordinated and uncoordinated water molecules is obtained.

References

(1) K. Nakamoto, *Infrared and Raman Spectra of Inorganic and Coordination Compounds,* 3rd ed., (John Wiley, New York, 1978).

(2) J. A. Pople, W. G. Schneider, and H. J. Bernstein, *High Resolution Nuclear Magnetic Resonance,* (McGraw-Hill, New York, 1959).

(3) A. Abragam, *The Principles of Nuclear Magnetism,* (Oxford University Press, Oxford, 1961).

(4) P. Pottel, *Water, A Comprehensive Treatise,* edited by F. Franks, (Plenum Press, New York, 1973), Vol. 3, Chapter 8.

(5) H. Ohtaki, *Rev. Inorg. Chem.*, 4, 103 (1982).

(6) J. F. Hinton and E. S. Amis, *Chem. Rev.*, 67, 367 (1967).

(7) C. Deverell, *Prog. NMR Spectrosc.*, 4, 235 (1969).

(8) H. G. Hertz, *Water, A Comprehensive Treatise,* edited by F. Franks, (Plenum Press, New York, 1973), Vol. 3, Chapter 7.

(9) A. K. Covington and K. E. Newman, *Modern Aspects of Electrochemistry,* edited by J. O. Bockris and B. E. Conway, (Plenum Press, New York, 1977).

(10) R. G. Bryant, *Annu. Rev. Phys. Chem.*, 29, 167 (1978).

(11) J. Burgess, *Metal Ions in Solution,* (John Wiley, New York, 1978).

(12) M. C. R. Symons, *Pure Appl. Chem.*, 51, 1671 (1979).

(13) J. J. Dechter, *Prog. Inorg. Chem.*, 29, 285 (1982).

(14) H. G. Hertz, *Pure Appl. Chem.*, 54, 2297 (1982).

(15) M. Holz, *Prog. NMR Spectrosc.*, 18, 327 (1986).

(16) H. Fukui, K. Miura, T. Ugai, and M. Abe, *J. Phys. Chem.*, 81, 1205 (1977).

(17) K. Miura and H. Fukui, *Inorg. Chem.*, 19, 995 (1980).

(18) K. Miura, M. Tanaka, H. Fukui, and H. Toyama, *J. Phys. Chem.*, submitted to the editor.

(19) K. Miura, K. Hashimoto, H. Fukui, E. Yamada, and S. Shimokawa, *J. Phys. Chem.*, 89, 5098 (1985).

Chapter II

Ion-Water Interaction

1 Introduction

Water proton magnetic resonance chemical shifts produced by diamagnetic salts in aqueous solution have been used to study the effects of electrolytes on the structure of water and the nature of solute-solvent interaction.[1-7] In dilute solutions the observed shift was related to the aqueous molal salt shifts.[8] According to Schoolery and Alder,[1] the chemical shift produced by ions in aqueous solution is the superposition of at least two factors: (i) polarization of water molecules and (ii) structure breaking of the water hydrogen-bonded network. The interaction between a cation and a water molecule through the oxygen atom produces a shift in electron density away from the protons, leaving them less shielded. Therefore, relative to pure water, the resonance occurs at a lower field strength. It was also reasoned that the interaction between an anion and a water molecule would produce a similar lower field shift due to the attraction of the proton for the anion; the electron cloud around the hydrogen atom again being shifted toward the oxygen atom owing to repulsion by the anion. One must also consider the case in which the water proton might become embedded in the

electron cloud of a large anion. In this case the proton becomes more shielded and resonates at a higher field relative to that in pure water. These effects would constitute the polarization shift by a salt. Ions breaking the water hydrogen-bond structure would produce high-field shifts due to the increased electron density around the protons. The polarization effect and the structure-breaking effect produce generally shifts in the opposite direction, and are of the same order of magnitude.

If we want to investigate the mechanism of the shielding change due to the hydration of ions, it is desirable to separate the above two contributions. Therefore, I have focused attention on the magnitudes of the shifts produced by the polarization effect alone. In order to eliminate the structure-breaking effect, it is necessary to observe the water proton chemical shifts induced by salts in an inert solvent.[9-11] If the structure-breaking effect is negligible, or it can be evaluated, then the direct salt-molecular polarization shift is accessible to experimental observation. If we use solutions of extremely low water content to eliminate water to water hydrogen bonding, the structure-breaking effect would be negligible. Then we have to use time averaging of the water proton signal to observe chemical shift changes. In order to avoid this cumbersome measurement,

we may observe the chemical shift at an appropriately low water concentration, and correct the observed polarization shift to give the shift from the zero water concentration by adding the dilution shift. Moreover, it is possible to observe a favorable one-to-one complex formation at low water concentrations in an inert solvent.[9,10] The 1:1 complex formation allows us to analyze the chemical shift changes and obtain the polarization shift and equilibrium constant. Stockton and Martin[10] observed and analyzed the 1:1 association of several metal ions with a water molecule in 0.1 M water-acetonitrile solutions at room temperature. They obtained the polarization shifts and hydration constants of Li^+, Na^+, Mg^{2+}, Ca^{2+}, Sr^{2+}, and Ba^{2+} in acetonitrile. Benoit and Lam[11] used similar experimental conditions and estimated the polarization shifts and the water association constants of Cl^-, NO_3^-, Li^+, Na^+, and Ag^+ in several dipolar aprotic solvents.

It is known that the molal salt shift can be written as the sum of the individual cation and anion molal shifts.[1] The salt shifts were divided into individual ion values, assuming some value for one ion to be used as a standard.[8,12-14] However, there have not yet been any studies of the additivity of the polarization salt shift. Stockton and Martin[10] and Benoit and Lam[11] used perchlorate and tetraethylammonium salts to minimize counterion

contributions. It is of fundamental importance to know how the extent of hydration is affected by the counterion. In this chapter, I will report on the polarization shifts and the hydration constants of various ions, and discuss the additivity of the former. I will also investigate relationships of the polarization ion shift and the hydration constant to the ionic size.

Stockton and Martin[10] used acetonitrile as an inert solvent. It is available in perdeuterated form, which does not obscure the spectral region of interest. I have used acetone as an inert solvent and it does not overlap the water proton signal. Fratiello et al.[15] indicated that the solvating ability of acetone is comparable to that of acetonitrile. From this fact, it is inferred that acetone is as inert as acetonitrile. The water concentration was kept as low as possible (0.1 M) to minimize water to water hydrogen bonding, and the water proton shielding was observed as a function of salt concentration.

2 Experiment

Materials. Wako Pure Chemicals acetone was distilled twice from a freshly dehydrated 4A molecular sieve. The residual water concentration in the acetone thus obtained was about 0.004 M. Tetramethylsilane (TMS) was added before the sample preparation to serve as a ^{1}H NMR

internal reference.

Water was distilled and passed over cation- and anion-exchange resins.

Calcium and strontium perchlorates were hexahydrates; they were dehydrated by heating at 100°C under vacuum pumping, gradually increasing to 200°C over several days. Lithium, sodium, magnesium, and barium perchlorates were obtained labeled "anhydrous" and were dried by heating at 200°C under vacuum pumping.

The lithium and calcium thiocyanates obtained were anhydrous and trihydrate, respectively; they were dehydrated by heating at 100°C under vacuum for 48 h.

Calcium nitrate was in the tetrahydrate form; it was dehydrated by heating at 125°C under vacuum for 48 h. Lithium nitrate was obtained labeled anhydrous and was dried by heating.

The lithium iodide obtained was labeled anhydrous, however it contained traces of water. Attempts to dehydrate it by heating under vacuum yielded a sample containing a slight amount of water. Lithium bromide was monohydrate; it was dehydrated by heating at 190°C under vacuum for 24 h.

The cadmium nitrate was tetrahydrates; it was dehydrated by heating at 60°C under vacuum for 24 h, gradually increasing to 120°C over 24 h.

The zinc chloride and bromide, mercuric, stannous, and antimony chlorides, and cadmium iodide that were obtained were labeled anhydrous and were dried by heating.

The ^{1}H NMR spectrum of the reagent grade tetra-*n*-butylammonium chloride showed a slight impurity signal. The salt was dissolved in a small volume of CCl_4, then precipitated by adding cyclohexane. The salt so obtained was then dried by pumping and found by ^{1}H NMR to be free from impurities. The tetra-*n*-butylammonium bromide, iodide, and perchlorate were used as received, since no ^{1}H NMR impurity signals (dissolved in acetone) were observed.

Solutions of 0.1 M water–acetone, with varying salt concentrations over the range 0 to about 1 M, were prepared. All samples were made up gravimetrically.

^{1}H NMR Spectra. All spectra were obtained on a Hitachi R-20A spectrometer (permanent magnet, 60 MHz). All measurements were made at 34±1°C. Downfield shifts were taken as positive.

3 Analysis

Analysis of the Observed Shift. My approach to the problem was to measure the ^{1}H NMR chemical shift of water in acetone, relative to some reference, as a function of concentration of added salt. Only one water ^{1}H NMR peak was observed in these solutions, indicating that exchange of

H_2O molecules occurs so rapidly from one state to another that the observed chemical shift is an average of all the states. It is impossible, however, to know exactly all the states. For simplicity I consider only two states of water: the free and complexed forms. I consider only the reaction

$$IS_n + H_2O \rightleftarrows IS_{n-1}H_2O + S \qquad (1)$$

where I and S are an ion and a solvent (acetone in this experiment) molecule, respectively.[16] I assumed the following in eq 1: (i) either the cation or the anion contributes to the complex formation with H_2O and (ii) one water molecule exchanges with one solvent molecule. The observed chemical shift δ is given by the equation

$$\delta = \frac{[F]}{W_0}\delta_F + \frac{[C]}{W_0}\delta_C \qquad (2)$$

where W_0 is the initial concentration of H_2O (0.1 M in this experiment), [F] and [C] are the equilibrium concentrations of the free and complexed water, respectively, and δ_F and δ_C are the characteristic chemical shifts of those forms of water. The concentration of solvent is so large that it is constant in eq 1. The equilibrium constant K of reaction 1 is given by

$$K = \frac{[C]}{(I_0-[C])(W_0-[C])} \qquad (3)$$

where I_0 is the initial concentration of the reactive ion. We define the complex formation shift Δ_C as

$$\Delta_C = \delta_C - \delta_F \qquad (4)$$

Equations 2 and 4 yield

$$\delta = \delta_F + \frac{[C]}{W_0}\Delta_C \qquad (5)$$

At the limit of high concentration of the ion, $\delta-\delta_F$ is equal to the complex shift Δ_C. Analyses of the observed shifts were performed using a computer simulation method.[17] In most cases analyses of the data yielded sufficiently reliable values of K and Δ_C. The mechanism of the shielding change as pictured here is undoubtedly over-simplified; nevertheless, it provides a tentative working scheme which appears to be in agreement with the facts available.

4 Results and Discussion

(A) *Dilution Shift of Water in Acetone*

The dilution shift of water in acetone from 0.1 M to zero concentration was estimated. Figure 1 shows the

concentration dependence of the water proton chemical shift in acetone from 0.01 to 0.25 M. The region below about 0.15 M is nearly linear. It is evident that extrapolation to infinite dilution gives 0.02 ppm as the dilution shift for the 0.1 M water-acetone solution. It is apparent that this value is within the experimental and analytical errors of the complex shift Δ_C, so I neglected the correction due to the dilution shift. We may assume that the complex shift Δ_C obtained in 0.1 M water-acetone solution is equal to the polarization shift.

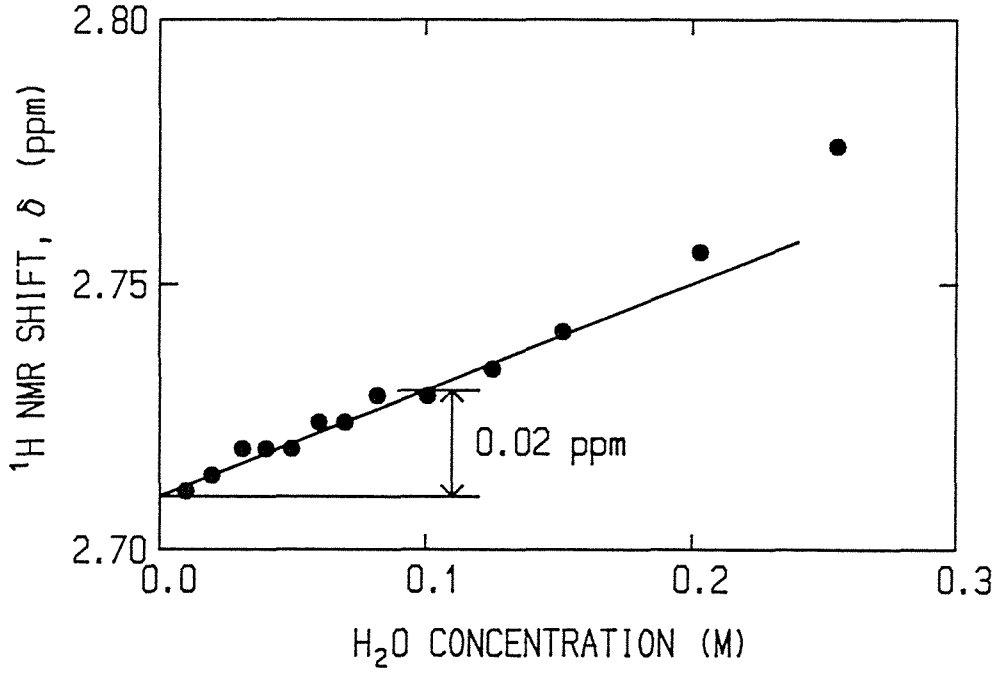

Figure 1. Dilution curve for the water proton chemical shift in acetone.

(B) *Cation Shifts in Metal Perchlorate Solutions*

The chemical shifts of the water proton signal in the alkali and alkaline earth perchlorate solutions were measured as a function of salt concentration. The effects of alkali and alkaline earth perchlorate salts on the water proton signal in acetone are shown in Figures 2-7, with the simulated curves. I supposed in the analysis that the perchlorate ion is inert and only a metal ion forms a 1:1 complex with a water molecule. Agreement between the observed and calculated shifts, except for the water -magnesium complex, were so good that the assumption of 1:1 association was confirmed. The equilibrium constants, the complex shifts of cations, and the standard deviations between observed and calculated shieldings, obtained by least-squares computer simulation, are listed in Table I with the results reported by Stockton and Martin.[10] The water-magnesium system showed evidence of multiple water-ion association at low salt concentrations, in which a large discrepancy occurred between the observed and simulated shieldings. The equilibrium constant for this system is listed only as "large" since it was not able to be determined from the concentration dependence of the shift.

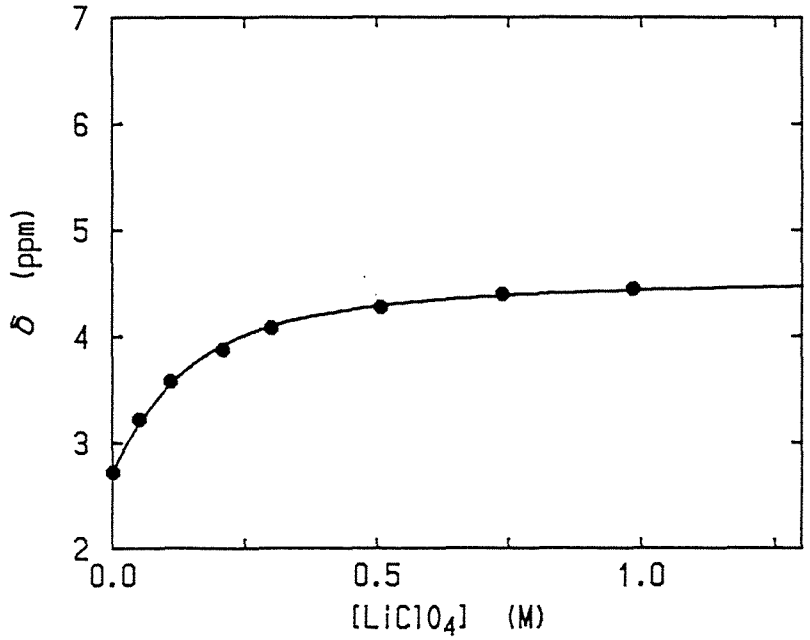

Figure 2. ^{1}H NMR shifts of the water proton in acetone solutions containing 0.1 M water and varying concentrations of $LiClO_4$: solid curve, simulated; closed circles, observed.

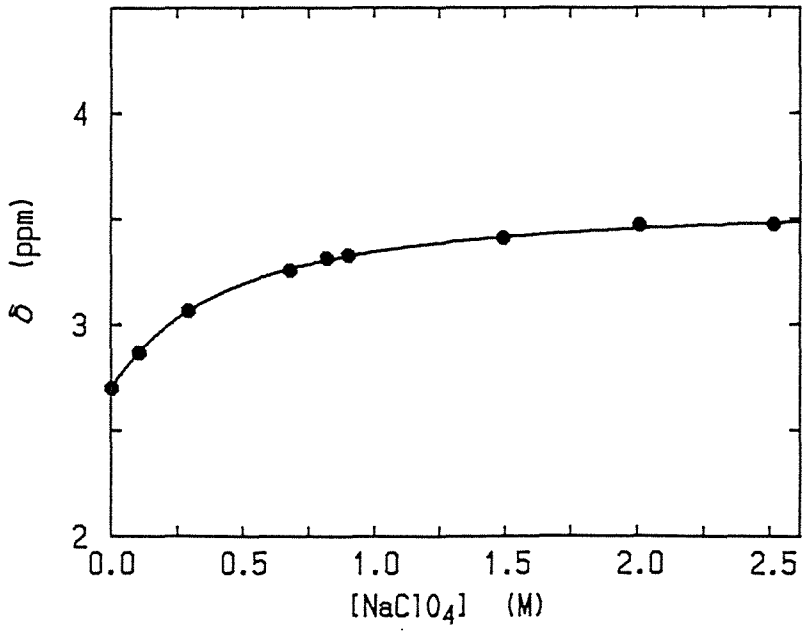

Figure 3. ^{1}H NMR shifts of the water proton in acetone solutions containing 0.1 M water and varying concentrations of $NaClO_4$: solid curve, simulated; closed circles, observed.

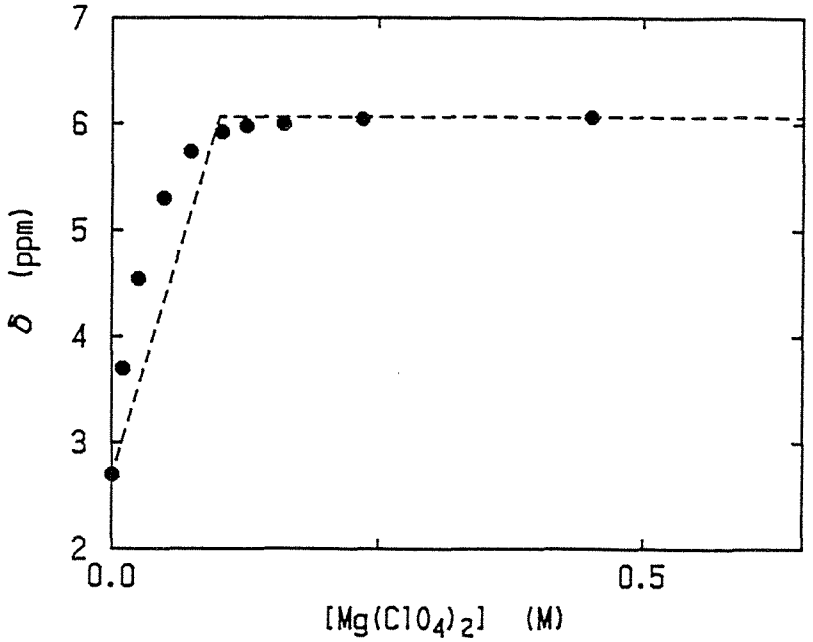

Figure 4. ^{1}H NMR shifts of the water proton in acetone solutions containing 0.1 M water and varying concentrations of $Mg(ClO_4)_2$: closed circles, observed.

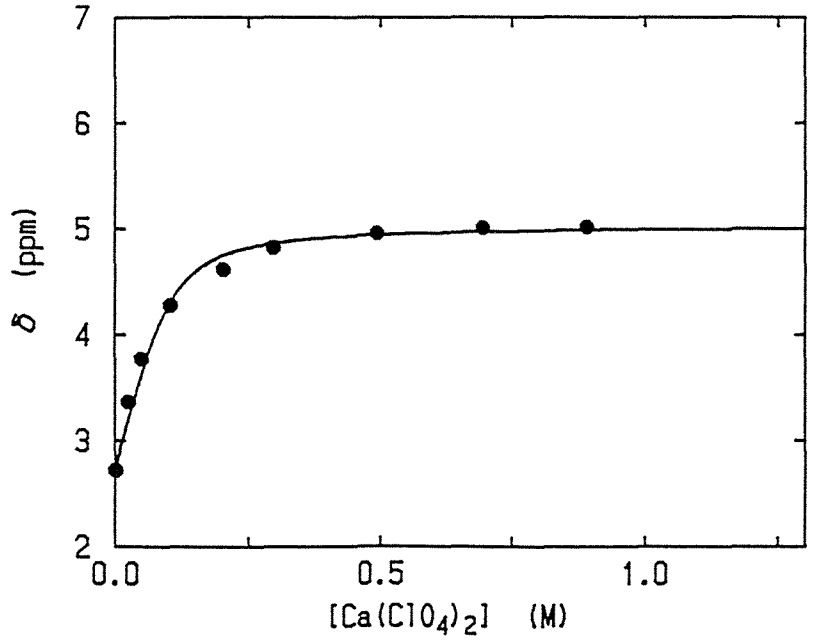

Figure 5. ^{1}H NMR shifts of the water proton in acetone solutions containing 0.1 M water and varying concentrations of $Ca(ClO_4)_2$: solid curve, simulated; closed circles, observed.

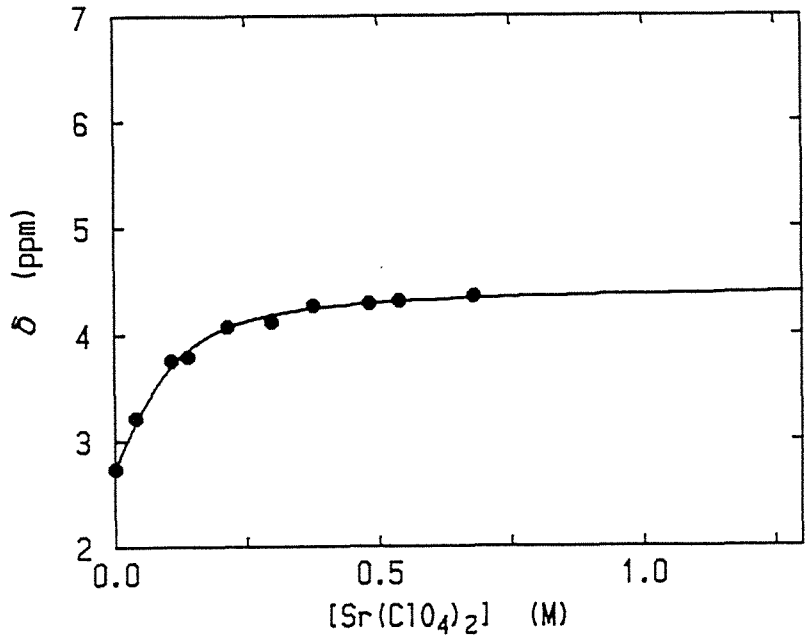

Figure 6. ^{1}H NMR shifts of the water proton in acetone solutions containing 0.1 M water and varying concentrations of $Sr(ClO_4)_2$: solid curve, simulated; closed circles, observed.

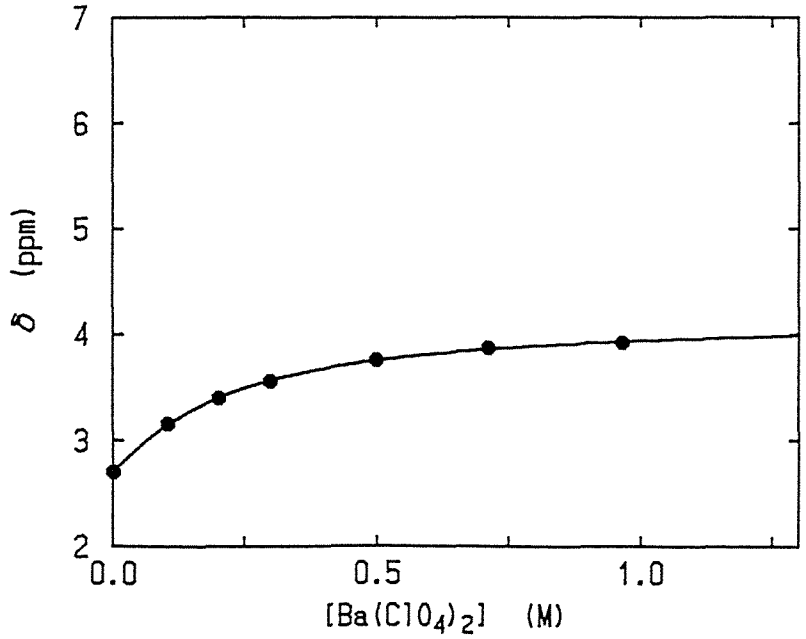

Figure 7. ^{1}H NMR shifts of the water proton in acetone solutions containing 0.1 M water and varying concentrations of $Ba(ClO_4)_2$: solid curve, simulated; closed circles, observed.

TABLE I. Equilibrium Constants K and Polarization Shifts Δ_C of Alkali and Alkaline Earth Perchlorates in Acetone at 34°C, with the Results Reported by Stockton and Martin[10].

Salt	K (M^{-1})		Δ_C (ppm)	
$LiClO_4$	12 ± 1	14[a]	1.87±0.04	1.48[a]
$NaClO_4$	2.8± 0.2	2.3[a]	0.90±0.01	0.89[a]
$Mg(ClO_4)_2$	Large	Large[a]	3.36	2.98[a]
$Ca(ClO_4)_2$	63 ±22	151[a]	2.31±0.07	2.17[a]
$Sr(ClO_4)_2$	28 ± 5	45[a]	1.71±0.04	1.75[a]
$Ba(ClO_4)_2$	6.0± 0.4	16[a]	1.47±0.03	1.54[a]

[a] Reported by Stockton and Martin[10] in acetonitrile at 35°C.

It is evident from Table I that ions of smaller size or larger charge have larger equilibrium constants and complex shifts. This will be discussed later (section E). It is shown that the polarization shifts obtained in acetone are in agreement with those in acetonitrile.[10] Stockton and Martin[10] have asserted that cation-induced shifts should be independent of the solvent. My experiments support

their assertion. However, the equilibrium constants in acetone are smaller than those in acetonitrile which seems to indicate that the solvating ability of acetone is slightly greater than that of acetonitrile.

(C) *Anion Shifts in Tetra-n-butylammonium Salt Solutions*

In order to obtain the values K and Δ_C for anions, the chemical shifts produced by tetra-*n*-butylammonium halides and perchlorate were measured. In this case the tetra-*n*-butylammonium ion should be inert and only an anion can form a complex with H_2O. Figures 8-11 show the variations of measured shifts and simulated curves. The equilibrium constants and the complex shifts of anions were determined, and are listed in Table II. The polarization shifts of Cl^- and Br^- are somewhat large, but those of I^- and ClO_4^- are very small. The equilibrium constants show a less regular variation. From the polarization shifts, it is inferred that I^- and ClO_4^- do not associate with water, but Cl^- and Br^- do weakly. It is apparent from Δ_C for $(n\text{-}C_4H_9)_4NClO_4$ that both the perchlorate and tetra-*n*-butylammonium ions are inert.

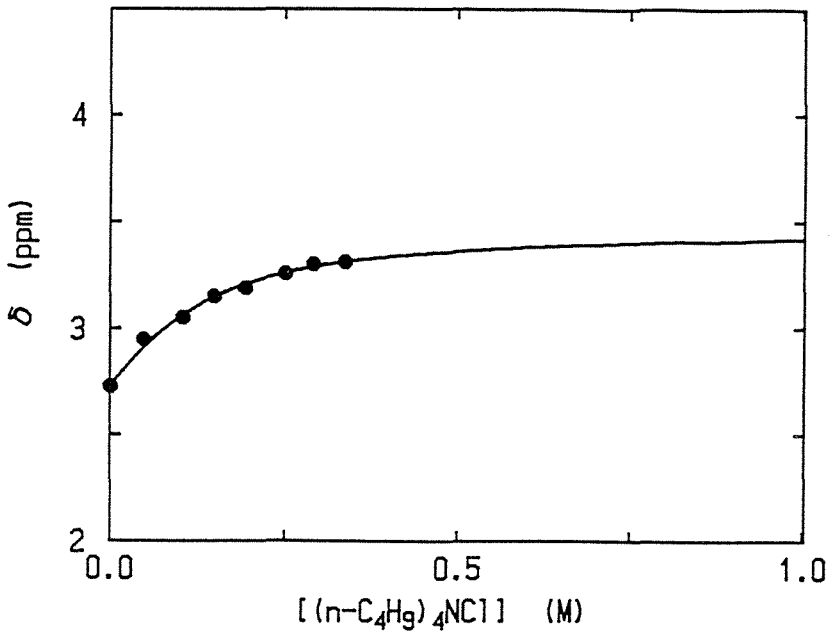

Figure 8. ^{1}H NMR shifts of the water proton in acetone solutions containing 0.1 M water and varying concentrations of $(n\text{-Bu})_4NCl$: solid curve, simulated; closed circles, observed.

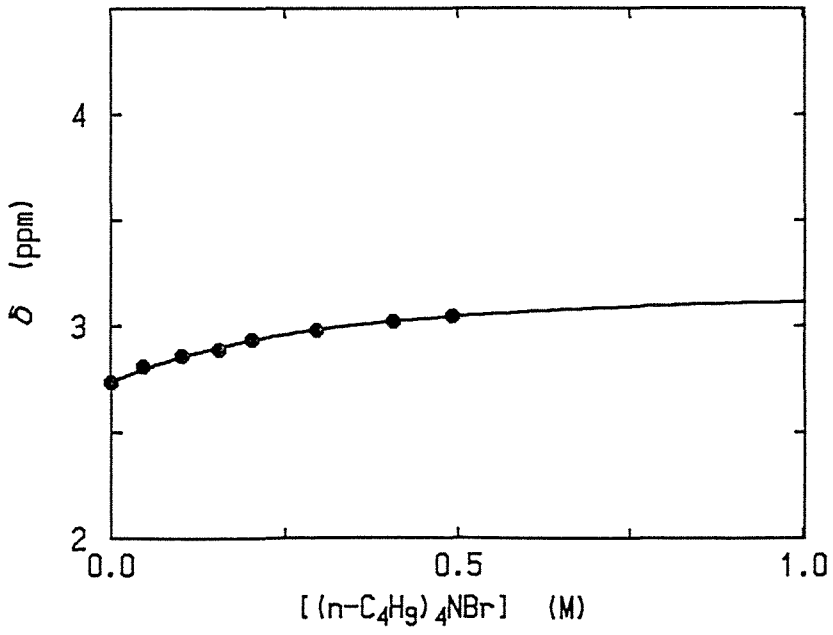

Figure 9. ^{1}H NMR shifts of the water proton in acetone solutions containing 0.1 M water and varying concentrations of $(n\text{-Bu})_4NBr$: solid curve, simulated; closed circles, observed.

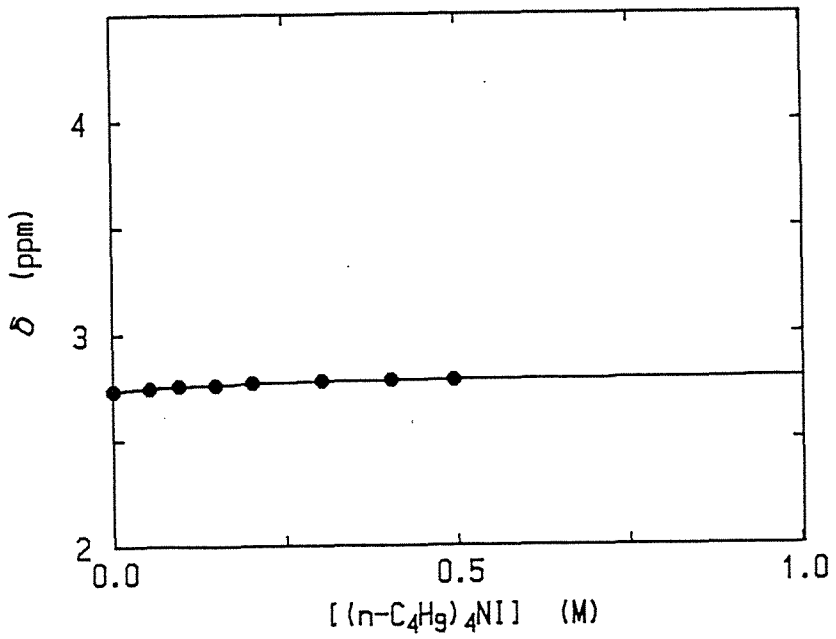

Figure 10. ^{1}H NMR shifts of the water proton in acetone solutions containing 0.1 M water and varying concentrations of $(n\text{-Bu})_4NI$: solid curve, simulated; closed circles, observed.

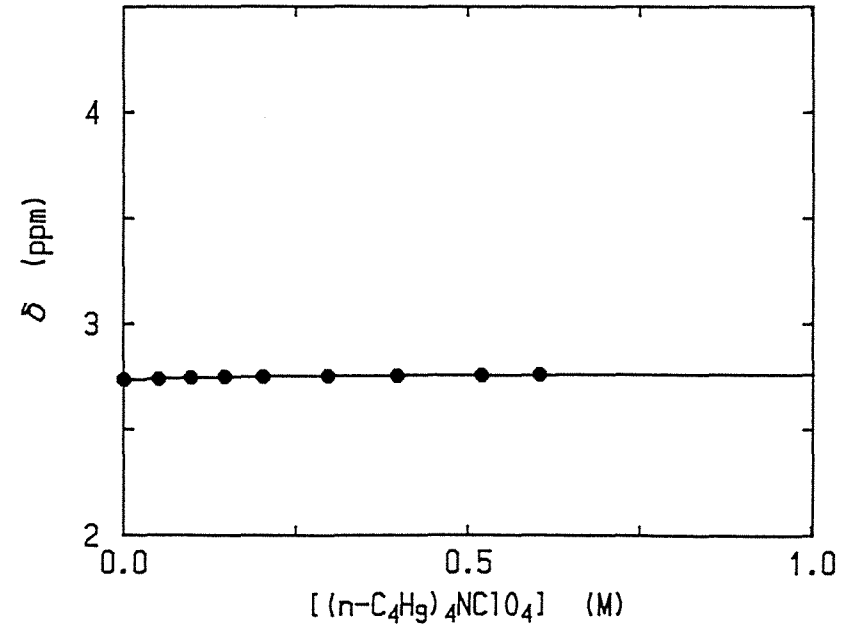

Figure 11. ^{1}H NMR shifts of the water proton in acetone solutions containing 0.1 M water and varying concentrations of $(n\text{-Bu})_4NClO_4$: solid curve, simulated; closed circles, observed.

TABLE II. Equilibrium Constants and Polarization Shifts of Tetra-*n*-butylammonium Halides and Perchlorate in Acetone at 34°C.

Salt	K (M^{-1})	Δ_C (ppm)
$(n\text{-}C_4H_9)_4NCl$	14 ±4	0.75±0.05
$(n\text{-}C_4H_9)_4NBr$	4.5±0.8	0.47±0.03
$(n\text{-}C_4H_9)_4NI$	6.4±3.0	0.06±0.01
$(n\text{-}C_4H_9)_4NClO_4$	7.8±4.2	0.03±0.00

(D) *Anion Effects on Equilibrium Constant and Complex Shift*

It is reported that the molal salt shift is the sum of the individual ion values.[1] However, at present no reports are available on the additivity of the polarization shift, so I have attempted to study this additivity. It is desirable to investigate the complex shifts of salts having various anions for specific cation or vice versa. The kinds of salts studied were limited by the solubilities of salts and the difficulty in obtaining anhydrous salts. I report here on lithium, calcium, zinc, and cadmium salts.

The variations of shifts except for perchlorate salts are shown in Figures 12-21. The results are listed in Table III. In these experiments, both the cation and anion have the possibility to complex with water. Nevertheless, the experimental results showed that either cation or anion is bound to water, and the assumption (i) in the analysis section is valid for these salts.

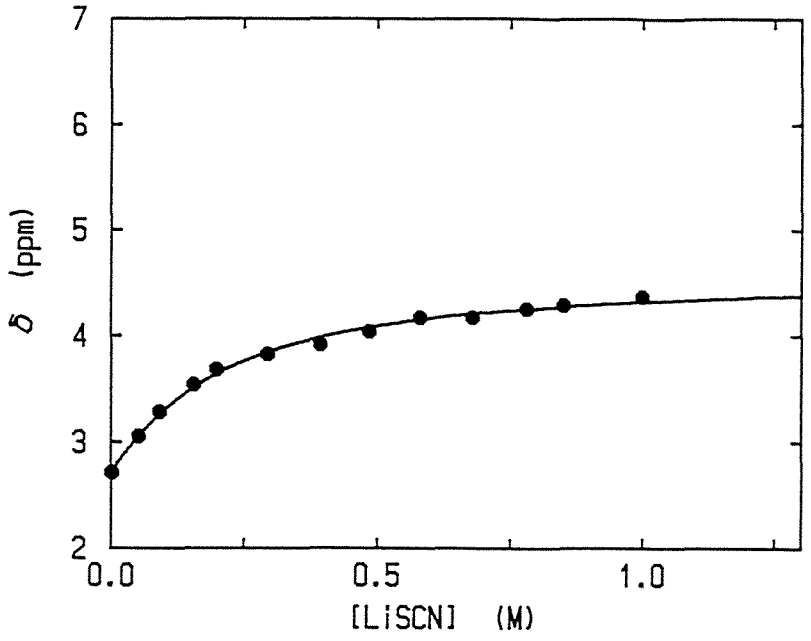

Figure 12. ^{1}H NMR shifts of the water proton in acetone solutions containing 0.1 M water and varying concentrations of LiSCN: solid curve, simulated; closed circles, observed.

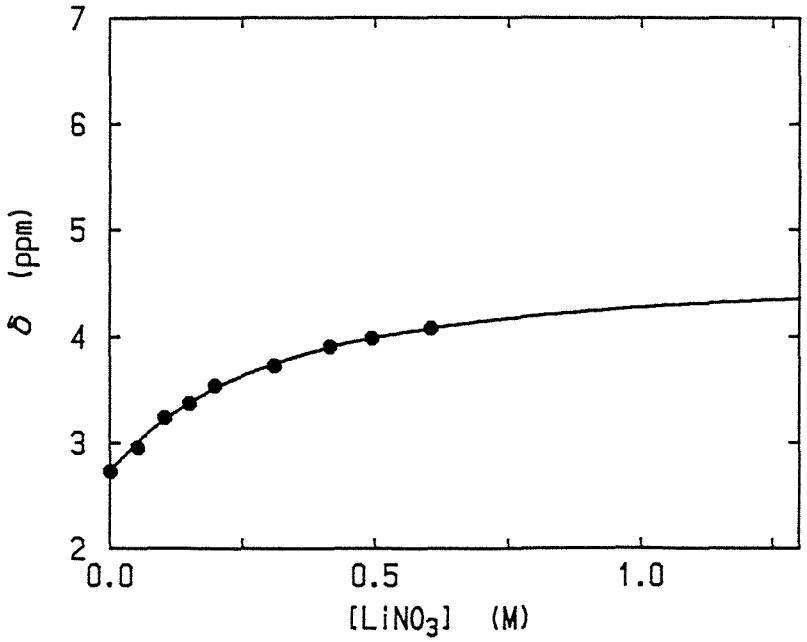

Figure 13. ^{1}H NMR shifts of the water proton in acetone solutions containing 0.1 M water and varying concentrations of $LiNO_3$: solid curve, simulated; closed circles, observed.

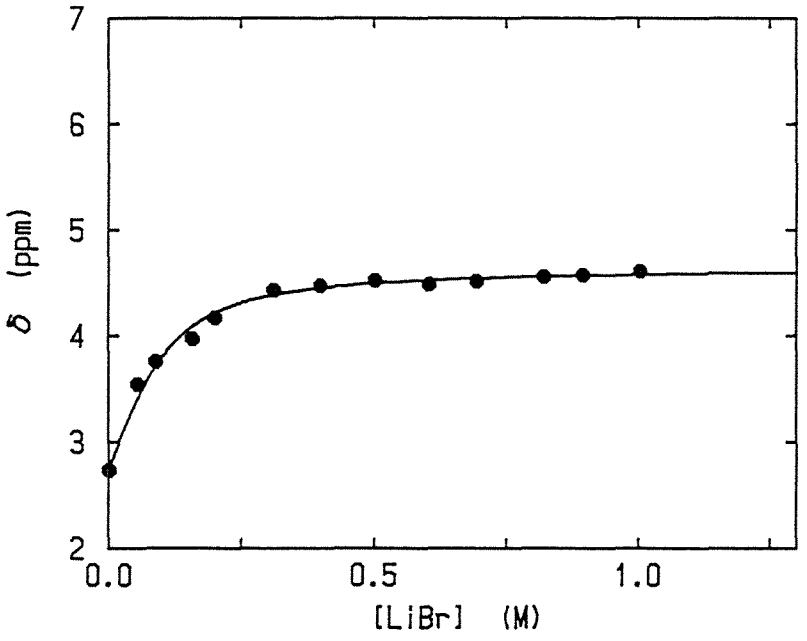

Figure 14. ^{1}H NMR shifts of the water proton in acetone solutions containing 0.1 M water and varying concentrations of LiBr: solid curve, simulated; closed circles, observed.

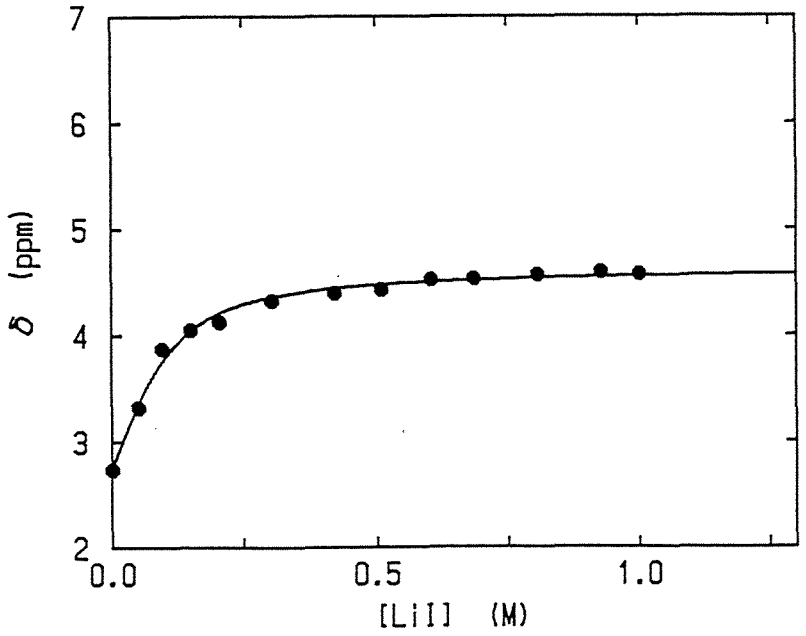

Figure 15. ^{1}H NMR shifts of the water proton in acetone solutions containing 0.1 M water and varying concentrations of LiI: solid curve, simulated; closed circles, observed.

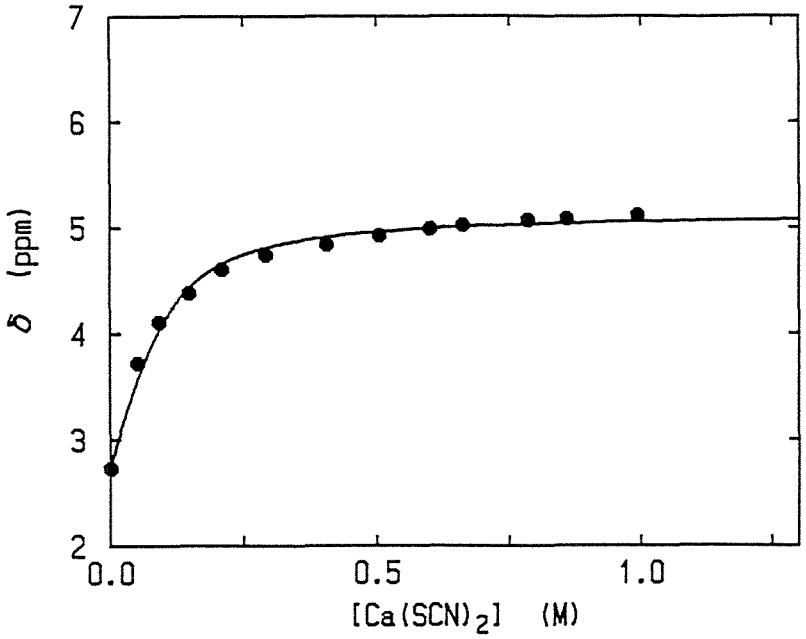

Figure 16. ^{1}H NMR shifts of the water proton in acetone solutions containing 0.1 M water and varying concentrations of $Ca(SCN)_2$: solid curve, simulated; closed circles, observed.

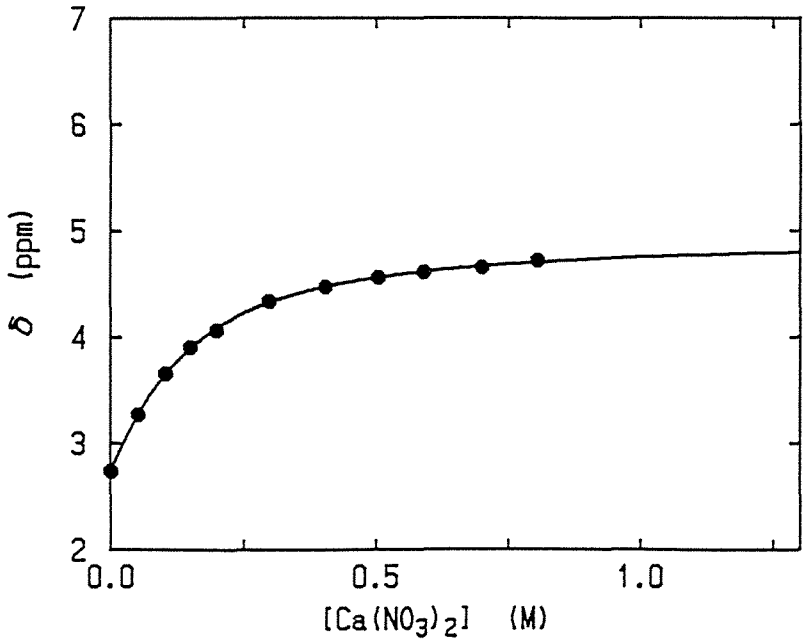

Figure 17. ^{1}H NMR shifts of the water proton in acetone solutions containing 0.1 M water and varying concentrations of $Ca(NO_3)_2$: solid curve, simulated; closed circles, observed.

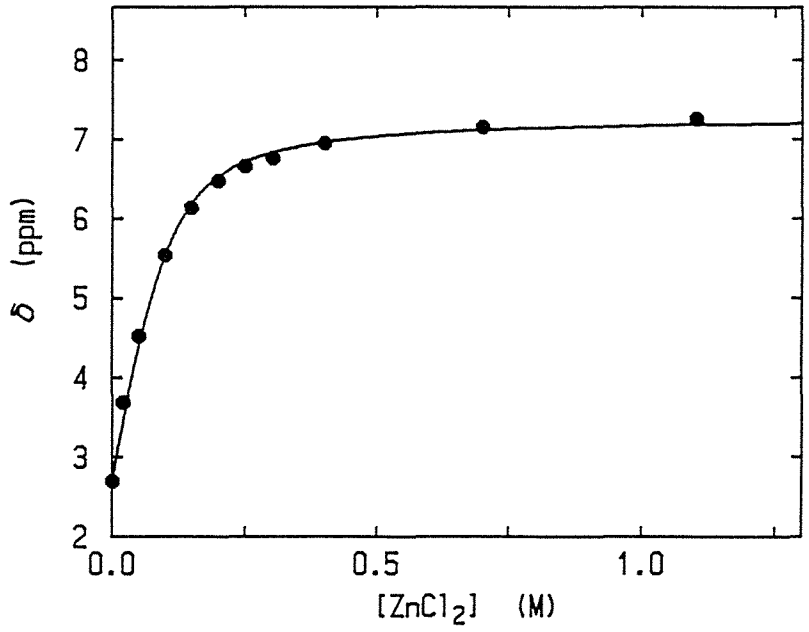

Figure 18. ^{1}H NMR shifts of the water proton in acetone solutions containing 0.1 M water and varying concentrations of $ZnCl_2$: solid curve, simulated; closed circles, observed.

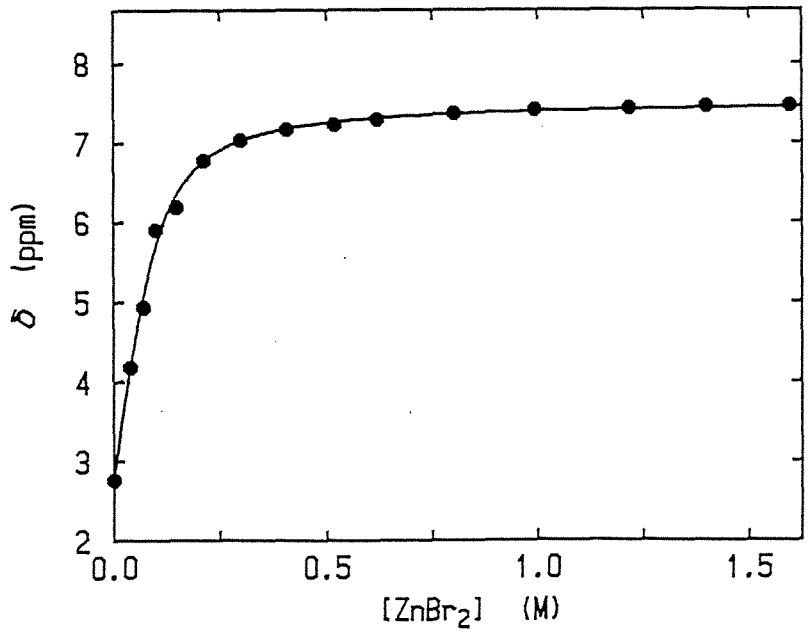

Figure 19. ^{1}H NMR shifts of the water proton in acetone solutions containing 0.1 M water and varying concentrations of $ZnBr_2$: solid curve, simulated; closed circles, observed.

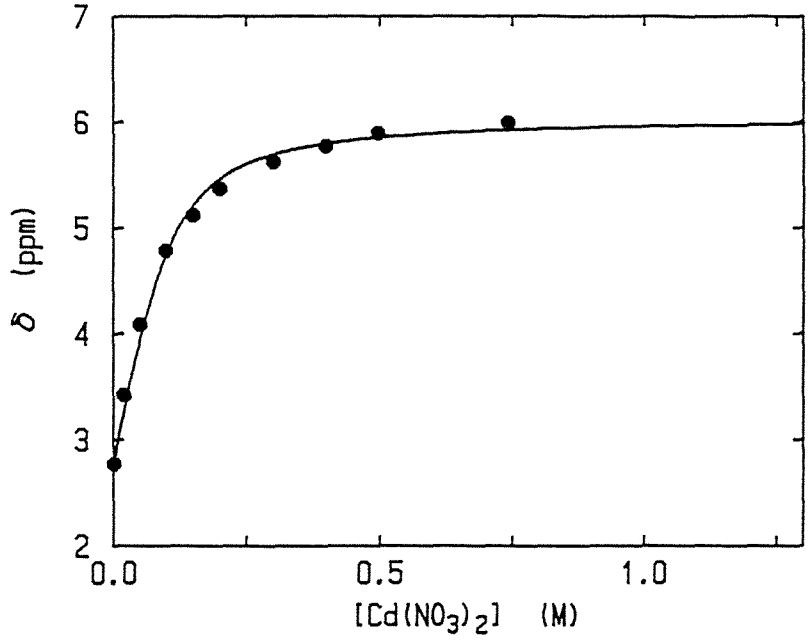

Figure 20. ^{1}H NMR shifts of the water proton in acetone solutions containing 0.1 M water and varying concentrations of $Cd(NO_3)_2$: solid curve, simulated; closed circles, observed.

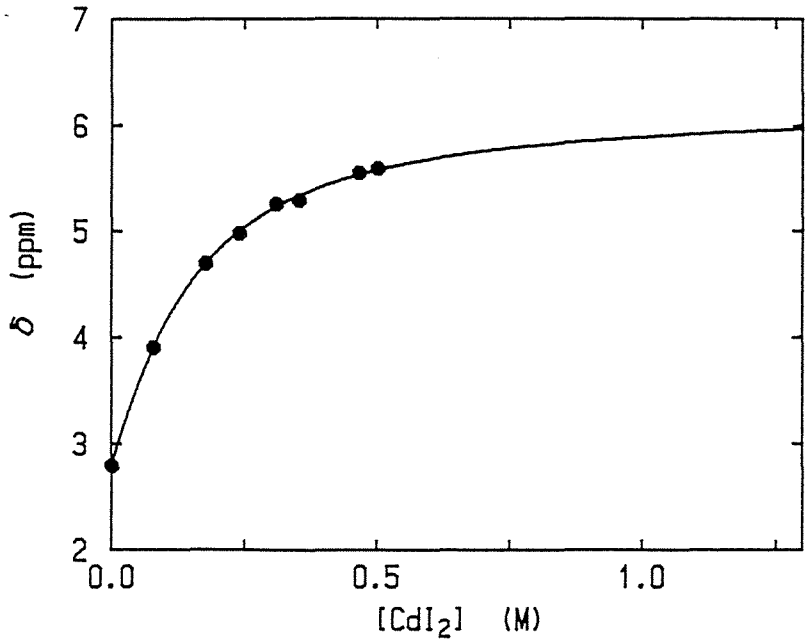

Figure 21. ^{1}H NMR shifts of the water proton in acetone solutions containing 0.1 M water and varying concentrations of CdI_2: solid curve, simulated; closed circles, observed.

TABLE III. Anion Dependence of Equilibrium Constants and Polarization Shifts of Lithium, Calcium, Zinc, and Cadmium Salts in Acetone at 34°C.

Cation	Anion	K (M^{-1})	Δ_C (ppm)
Li^+	ClO_4^-	12 ± 1	1.87±0.04
Li^+	SCN^-	6.4± 0.6	1.88±0.04
Li^+	NO_3^-	4.3± 0.5	1.93±0.09
Li^+	Br^-	28 ± 4	1.91±0.04
Li^+	I^-	28 ± 4[a]	1.89±0.03[a]
Ca^{2+}	ClO_4^-	62 ±22	2.31±0.07
Ca^{2+}	SCN^-	31 ± 4	2.41±0.04
Ca^{2+}	NO_3^-	11 ± 1	2.22±0.02
Zn^{2+}	Cl^-	43 ± 6	4.59±0.08
Zn^{2+}	Br^-	41 ± 4	4.76±0.04
Cd^{2+}	NO_3^-	39 ± 8	3.28±0.08
Cd^{2+}	I^-	10 ± 1	3.44±0.09

[a] Lithium iodide contained a slight amount of water.

The anion dependence of the equilibrium constants and polarization shifts, given in Table III, are very interesting. The polarization shifts in Table III show little variation with the anion. For a given cation, all the metal salts have shown the same polarization shift within the experimental error. It seems that the polarization shift of a metal salt is primarily determined by the metal ion and the anion has a negligible effect on it. Notwithstanding the limited data, it is reasonable to suppose that a water molecule in metal salt solutions forms a complex with a metal ion, but not with an anion. It was shown that the anion in tetra-*n*-butylammonium salt solutions can weakly coordinate to a water molecule, but the anion in metal salt solutions cannot be bound to water. This means that either cation or anion in salt solutions, namely only the ion having a larger ability of coordination, can form a complex with a water molecule. Therefore, we can conclude that the additivity does not hold for the polarization shift.

However, the equilibrium constants are greatly affected by the anions, which seems to contradict the results for the polarization shifts. I cannot explain exactly the differences in K values. One can only attribute these differences to (i) failure to maintain constant ionic strength and (ii) the interaction between the cation and

anion spheres.

(E) *Correlation with Crystal Radius*

The values of the equilibrium constants and polarization shifts in Table I show that they are closely related to the ionic sizes and ionic charges of the cations. This suggests that K and Δ_C of the alkali and alkaline earth metal ions are determined by the electrostatic interaction between the ion and a water molecule. Figure 22 shows a plot of *log* K against $q/4\pi\varepsilon_0 r$, in which q is the ionic charge and r is the radius of ion. If, as is usually the case, the entropy changes of reaction 1 are either constant or proportional to the enthalpy changes, then *log* K should be linear in the electrostatic potential, $q/4\pi\varepsilon_0 r$. Figure 22 indicates that such a relationship does hold.

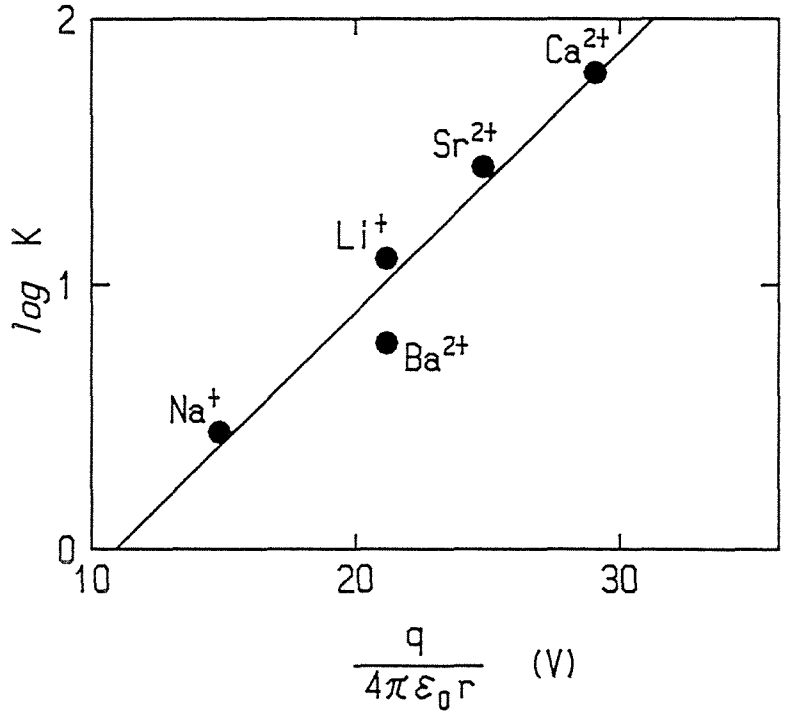

Figure 22. Relationship between the observed cation–water association constants and the electrostatic potential for the alkali and alkaline earth metal ions.

I have investigated the dependence of the polarization shifts on the electrostatic field of the cations. Assuming, for simplicity, that polarization shift is proportional to the electrostatic field,[18] Δ_C may be described as follows

$$\Delta_C = Aq/(4\pi\varepsilon_0(r+c)^2) \qquad (6)$$

where r+c is the distance from the ion center to the hydroxyl proton, and A is a proportionality factor. Equation 6 yields

$$r = (A/4\pi\varepsilon_0)^{1/2}(q/\Delta_C)^{1/2} - c \qquad (7)$$

If the shifts are proportional to the field, then r, the crystal radius, should be linear in $(q/\Delta_C)^{1/2}$. Figure 23 shows that such a relationship does hold for Δ_C in Table I. In this case I used the crystal radius[19] as the radius of ion. From the slope and intercept of the best straight line, I obtained $A=1.50\times10^{-17}$ $V^{-1}m$ and c=0.043 nm.

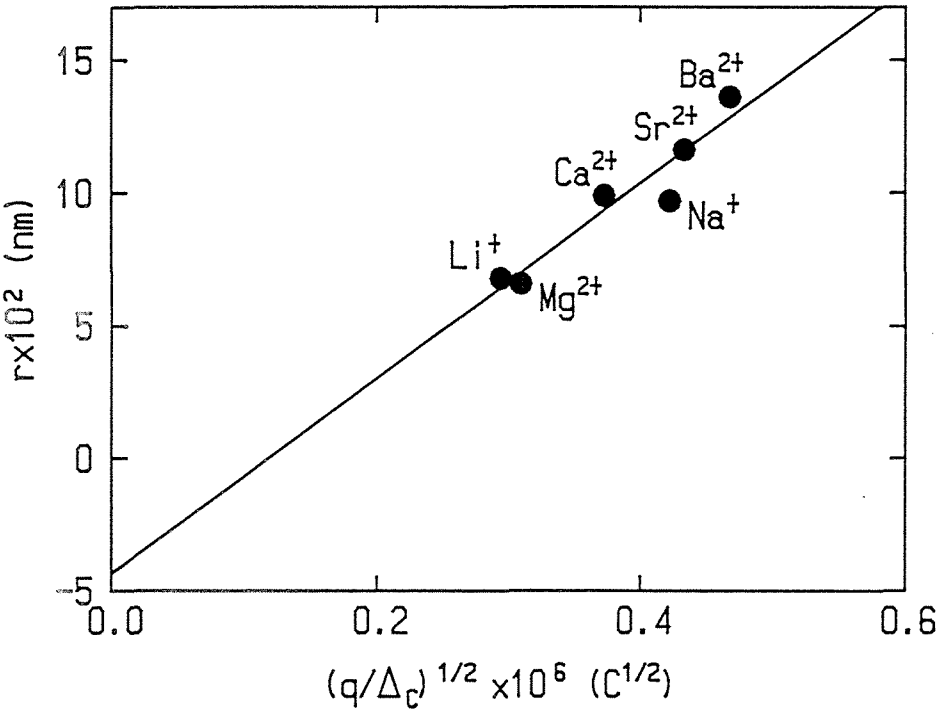

Figure 23. Relationship between the observed cation–water complex shifts and the crystal radii for the alkali and alkaline earth metal ions.

In order to examine further the correlation of K and Δ_C with the crystal radius, I measured water proton shifts and obtained K and Δ_C of metal ions other than alkali and alkaline earth metal ions, i.e., Hg^{2+}, Sn^{2+}, and Sb^{3+} ions. Figures 24-26 show the variations of chemical shifts. The results shown in Table IV indicate clearly that the linear relations, which were exhibited in Figures 22 and 23, do not hold any longer for cations other than the alkali and alkaline earth metal ions. For the similar plots for the anion shifts in Table II, I was not able to find only any relationships among r, Δ_C, and K. I conclude that K and Δ_C of the alkali and alkaline earth metal ions can be explained in terms of the electrostatic effect of the ion. However, those of the other metal cations and anions cannot be explained by the electrostatic model. This reflects the following: (i) the importance of covalent interactions for these ions and (ii) the possibility of ion pairing, which is common to ions of small size and large charge.

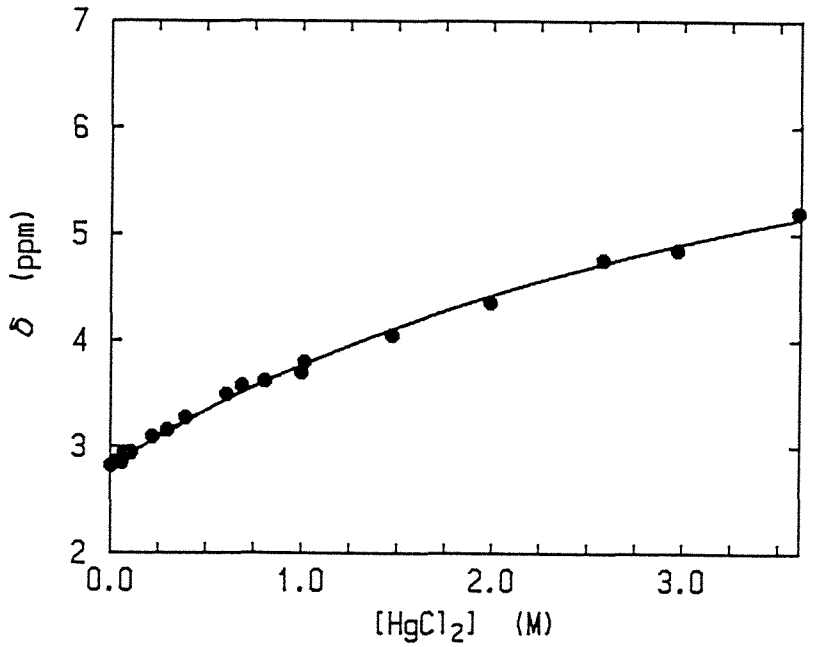

Figure 24. ^{1}H NMR shifts of the water proton in acetone solutions containing 0.1 M water and varying concentrations of $HgCl_2$: solid curve, simulated; closed circles, observed.

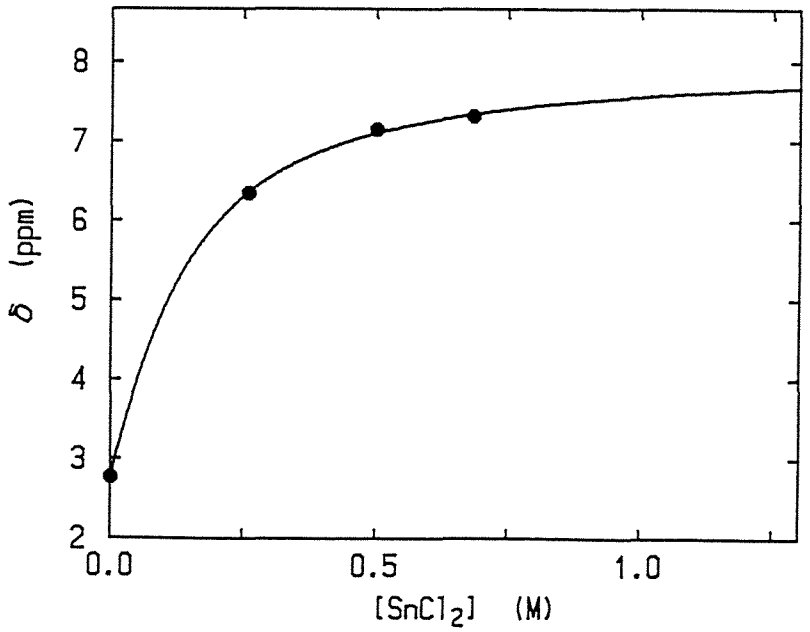

Figure 25. ^{1}H NMR shifts of the water proton in acetone solutions containing 0.1 M water and varying concentrations of $SnCl_2$: solid curve, simulated; closed circles, observed.

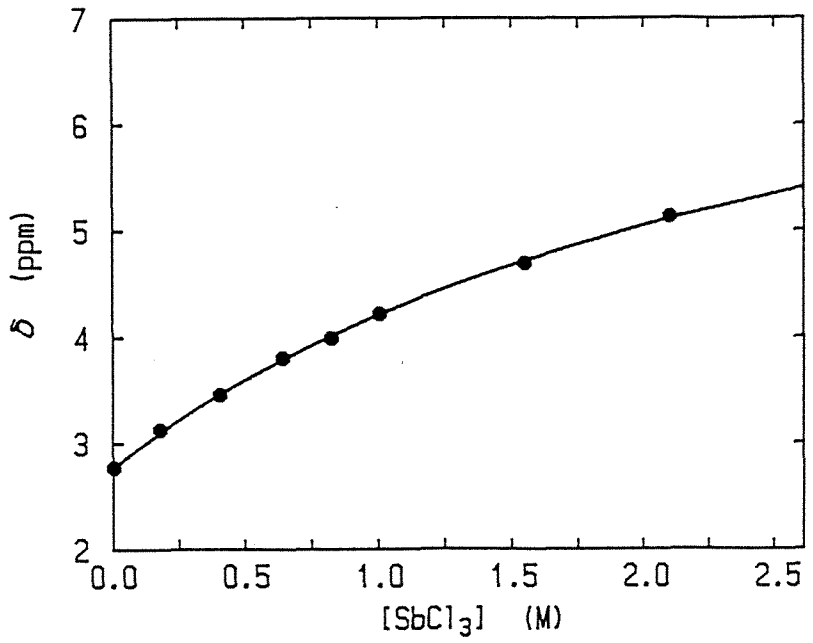

Figure 26. ^{1}H NMR shifts of the water proton in acetone solutions containing 0.1 M water and varying concentrations of $SbCl_3$: solid curve, simulated; closed circles, observed.

TABLE IV. Equilibrium Constants and Polarization Shifts of Various Metal Cations Other Than the Alkali and Alkaline Earth Metal Ions in Acetone at 34°C.

Cation	Salt	K (M^{-1})	Δ_C (ppm)
Zn^{2+}	$ZnCl_2$	43 ±6	4.59±0.08
Zn^{2+}	$ZnBr_2$	41 ±4	4.76±0.04
Cd^{2+}	$Cd(NO_3)_2$	39 ±8	3.28±0.08
Cd^{2+}	CdI_2	10 ±1	3.44±0.09
Hg^{2+}	$HgCl_2$	0.23±0.03	5.19±0.38
Sn^{2+}	$SnCl_2$	11 ±1	5.28±0.12
Sb^{3+}	$SbCl_3$	0.38±0.05	5.32±0.45

References

(1) J. N. Shoolery and B. J. Alder, *J. Chem. Phys.*, 23, 805 (1955).

(2) R. C. Axtmann, *J. Chem. Phys.*, 30, 340 (1959).

(3) H. G. Hertz and W. Spalthoff, *Z. Electrochem.*, 63, 1096 (1959).

(4) B. P. Fabricand and S. Goldberg, *J. Chem. Phys.*, 34, 1624 (1961).

(5) M. S. Bergqvist and E. Forslind, *Acta Chem. Scand.*, 16, 2069 (1962).

(6) J. C. Hindman, *J. Chem. Phys.*, 36, 1000 (1962).

(7) S. Goto and T. Isemura, *Bull. Chem. Soc. Jpn.*, 37, 1693 (1964).

(8) J. F. Hinton and E. S. Amis, *Chem. Rev.*, 67, 367 (1967).

(9) R. D. Green, J. S. Martin, W. B. M. Cassie, and J. B. Hyne, *Can. J. Chem.*, 47, 1639 (1969).

(10) G. W. Stockton and J. S. Martin, *J. Am. Chem. Soc.*, 94, 6921 (1972).

(11) R. L. Benoit and S. Y. Lam, *J. Am. Chem. Soc.*, 96, 7385 (1974).

(12) J. Davies, S. Ormondroyd, and M. C. R. Symons, *Trans. Faraday Soc.*, 67, 3465 (1971).

(13) J. Davies, S. Ormondroyd, and M. C. R. Symons, *J. Chem. Soc., Faraday Trans. II*, 686 (1972).

(14) M. C. R. Symons and J. Davies, *J. Chem. Soc., Faraday Trans. II*, 1037 (1975).

(15) A. Fratiello, R. E. Lee, D. P. Miller, and V. M. Nishida, *Mol. Phys.*, 13, 349 (1967).

(16) Kraus and co-workers estimated the dissociation constants of various salts in acetone at 25°C [M. B. Reynolds and C. A. Kraus, *J. Am. Chem. Soc.*, 70, 1709 (1948); M. J. McDowell and C. A. Kraus, *ibid.*, 73, 3293 (1951)], and found them to be of the order of 10^{-3}. It is suggested that the free ions would be only minor species. However, reaction 1 is not affected directly by the ion-pair reaction, because the distances d (nm) between centers of charge in the ion pairs are so large that each ion is surrounded on the average by a certain number of solvent molecules (e.g., for KI in acetone, 0.46 nm $\leq$ d $\leq$ 1.4 nm).

(17) S. Shimokawa, H. Fukui, J. Sohma, and K. Hotta, *J. Am. Chem. Soc.*, 95, 1777 (1973).

(18) A. D. Buckingham, *Can. J. Chem.*, 38, 300 (1960).

(19) L. Pauling, *The Nature of the Chemical Bond*, 3rd ed., (Cornell University Press, New York, 1960).

Chapter III

Theoretical Calculation for the Ion-Water Association Shift

1 Introduction

In Introduction of the previous chapter it was stated that the chemical shift produced by ions in aqueous solution is the superposition of at least two factors; (i) polarization of water molecules and (ii) structure breaking of the water hydrogen-bonded network, by ions.[1,2] If we want to investigate the mechanism of the shielding change due to the hydration of ions, it is desirable to separate the above two contributions. Fortunately, in Chapter II it was shown that the structure-breaking effect is experimentally negligible in the solution of low water content in acetone solvent.

A water molecule in acetone seems to form the hydrogen bond of water hydrogen to acetone oxygen. This hydrogen bonding will obstruct water-water and water-anion associations. Therefore, we can observe the shielding change owing to water-cation bonding only. Moreover, it is possible to observe a favorable 1:1 water-cation complex formation at low water concentrations in acetone solvent. The 1:1 complex formation allows us to analyze the chemical shift changes as a function of added ion concentration and

to obtain the polarization shift and equilibrium constant. However, the detailed relationship between proton magnetic shielding and the geometrical configuration of the hydrated ion system is not completely understood. This ambiguity places some uncertainty on conclusions resulting from the use of proton NMR spectroscopy for probing ion-water interactions. The purpose in this chapter is to perform an ab initio calculation of the shielding change of the water proton due to a point charge and compare it with the experimental results obtained in Chapter II.

2 Theory

When a molecular system including a nuclear magnetic moment $\vec{\mu}$ is placed in an external magnetic flux density $\vec{B}$, the electronic energy of the system has an additional nuclear magnetic energy proportional to $\vec{\mu}$ and $\vec{B}$, which is expressed as $\vec{\mu}\overleftrightarrow{\sigma}\vec{B}$ with the nuclear magnetic shielding tensor $\overleftrightarrow{\sigma}$. According to the Ramsey theory of chemical shielding,[3] the $\alpha\beta$ (α,β=x,y,z) component of the shielding tensor of nucleus N, $\sigma^{N}_{\alpha\beta}$, which produces the energy contribution bilinear in $\mu_{N\alpha}$ and B_{β}, is written as

$$\sigma^{N}_{\alpha\beta} = \sigma^{Nd}_{\alpha\beta} + \sigma^{Np}_{\alpha\beta} \qquad (\alpha,\beta=x,y,z) \qquad (1)$$

where $\sigma^{Nd}_{\alpha\beta}$ and $\sigma^{Np}_{\alpha\beta}$ are the components of the diamagnetic and paramagnetic terms, respectively. The diamagnetic

component $\sigma^{Nd}_{\alpha\beta}$, is given by

$$\sigma^{Nd}_{\alpha\beta} = 26.626 \times 10^{-6} \sum_{\mu\nu} P_{\mu\nu} \langle \mu | (\vec{r}_0 \cdot \vec{r}_N \delta_{\alpha\beta} - r_{0\alpha} r_{N\beta}) r_N^{-3} | \nu \rangle \quad (2)$$

where $\vec{r}_0$ denotes the vector from the gauge origin to an electron and $\vec{r}_N$ is the vector from nucleus N to the electron. The molecular coordinate is here taken as the coordinate system. r_0 and r_N are expressed in atomic units. The $\alpha\beta$ component of the paramagnetic shielding tensor, $\sigma^{Np}_{\alpha\beta}$, is given by, in atomic units,

$$\sigma^{Np}_{\alpha\beta} = 53.251 \times 10^{-6} \sum_{\substack{i,occ \\ j,unocc}} (\varepsilon_j - \varepsilon_i - J_{ij} + 2K_{ij})^{-1} \times$$

$$\sum_{\mu\nu\lambda\sigma} C^*_{\mu i} C_{\nu j} C^*_{\lambda j} C_{\sigma i} \{ \langle \mu | r_N^{-3} \ell_{N\alpha} | \nu \rangle \langle \lambda | \ell_{0\beta} | \sigma \rangle +$$

$$\langle \mu | \ell_{0\beta} | \nu \rangle \langle \lambda | r_N^{-3} \ell_{N\alpha} | \sigma \rangle \} \quad (3)$$

where $\vec{\ell}_0 = \vec{r}_0 \times \vec{\nabla}$ and $\vec{\ell}_N = \vec{r}_N \times \vec{\nabla}$. J_{ij} and K_{ij} are the molecular coulomb and exchange integrals, respectively.

Integrals of the following types occur in eqs 2 and 3: (i) $\langle \mu | r_N^{-3} x_0 y_N | \nu \rangle$; (ii) $\langle \mu | x_0 (\partial / \partial y_0) | \nu \rangle$; (iii) $\langle \mu | r_N^{-3} x_N (\partial / \partial y_N) | \nu \rangle$. Integral (ii) is quite easy to calculate. The other types of integrals, (i) and (iii), results in the evaluation of a $\langle \mu | r_N^{-3} x_N | \nu \rangle$ type integral. An integral of this type can be reduced to such field integrals as

$$\langle\mu|r_N^{-3}x_N|\nu\rangle = \frac{\partial}{\partial X_N}\langle\mu|r_N^{-1}|\nu\rangle \qquad (4)$$

where (X_N, Y_N, Z_N) is the coordinate of nucleus N. If we use the Gaussian type orbitals, the computation of the field integral requires no particular difficulty.

In a rapidly and isotropically rotating molecule in the liquid or gas phase, the nuclear magnetic energy, $\vec{\mu}\overleftrightarrow{\sigma}\vec{B}$, is averaged, and therefore only the averaged shielding tensor,

$$\sigma_N = \frac{1}{3}\sum_\alpha \sigma^N_{\alpha\alpha} \qquad (5)$$

is observed for nucleus N. σ_N is called the nuclear magnetic shielding constant of nucleus N, which is responsible for the isotropic chemical shift of nucleus N.

3 Method of Calculation

In a few attempts[4-6] to rationalize the shielding change in a static electric field, ab initio methods have been employed quite recently by some authors with success. This chapter is essentially aimed at investigating the ab initio predictions of the water proton and oxygen shielding changes due to an ionic field by using a point-charge model. The most difficult problem is always to get a reasonable compromise between the quality of a basis set and its size (computation time). In this calculation, Pople's 4-31G basis set[7] was used and a reasonable result was obtained.

For the H_2O molecular geometry I have used the experimental bond length and bond angle,[8] i.e., r_{OH}=0.0960 nm and ∠HOH=104.45°

In the computation of magnetic properties, further complications arise because of the gauge dependence of calculated values, which is due to the finite extension of the basis set, and some special choice of the gauge origin of the vector potential is commonly made in order to get an accurate paramagnetic contribution in susceptibility and shielding calculation. In this calculation, the oxygen nucleus was selected as the gauge origin in order to minimize the paramagnetic term.

All the calculations were performed on a FACOM 230-75 instrument at the Hokkaido University Computing Center.

4 Results and Discussion

(A) *Cation-Water Interaction Proton Shift*

The calculated shielding constants of the water proton due to a point charge are shown in Tables I and II, corresponding to univalent and divalent positive charges, respectively. Furthermore, the shielding changes are shown in Figure 1 as a function of the oxygen-positive point charge distance, r. On the basis of the X-ray diffraction study in solution,[9] the positive charge was set on the dipolar axis (C_2 axis) of the water molecule as drawn in

Figure 1.

TABLE I. Calculated Magnetic Shielding Constants of Proton in H_2O with the Distance r between Oxygen and Univalent Positive Point Charge.

r (nm)	σ^d (ppm)	σ^p (ppm)	σ (ppm)	$\Delta_C(calc)^a$ (ppm)
0.15	20.971	1.441	22.412	3.51
0.20	22.001	1.696	23.697	2.22
0.30	22.933	1.910	24.843	1.07
0.40	23.301	1.990	25.291	0.63
0.60	23.582	2.048	25.630	0.29
1.00	23.733	2.079	25.812	0.11
without charge	23.820	2.097	25.917	0.00

[a] $\Delta_C(calc)$ is defined as $\Delta_C(calc)=\sigma(\text{without charge})-\sigma(r)$.

TABLE II. Calculated Magnetic Shielding Constants of Proton in H_2O with the Distance r between Oxygen and Divalent Positive Point Charge.

r (nm)	σ^d (ppm)	σ^p (ppm)	σ (ppm)	Δ_C(calc) (ppm)
0.15	18.622	0.761	19.383	6.53
0.20	20.383	1.271	21.654	4.26
0.25	21.444	1.554	22.998	2.92
0.30	22.093	1.714	23.807	2.11
0.40	22.798	1.879	24.677	1.24
0.60	23.347	1.999	25.346	0.57
1.00	23.646	2.061	25.707	0.21
without charge	23.820	2.097	25.917	0.00

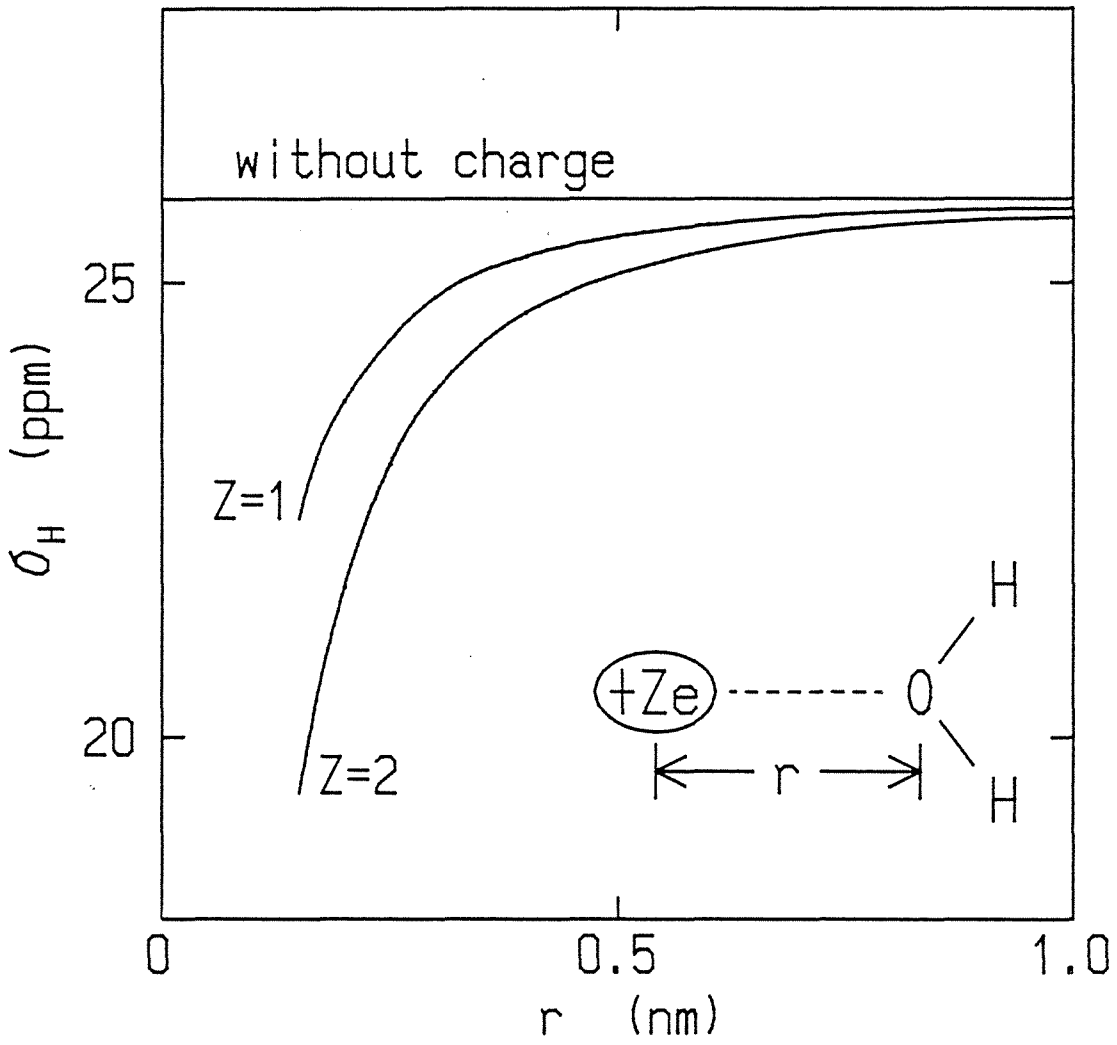

Figure 1. Variation of the calculated proton shielding constant in H_2O with the oxygen-positive point charge separation, r.

Figure 1 indicates that the calculated isotropic shielding constant of the water proton shows a marked decrease with decreasing of the distance r. An analysis of the theoretical results showed that the downfield proton shift due to ion hydration arises (a) from a decrease of the electronic charge on the hydrogen by an ionic field, i.e., σ^d effect and (b) from a deshielding effect of the paramagnetic contribution induced by an ion-water bonding, i.e., σ^p effect. The former contribution (a) is particularly important to cation hydration, in which the latter one (b) is only responsible for approximately 20% of the total calculated shielding change.

In Chapter II, it was concluded that the shielding change of the water proton, Δ_C, due to metal salt in acetone is primarily determined by the metal ion and the anion has a negligible effect on it. In order to investigate the cation shifts, I have performed a theoretical estimation for the shielding changes due to cations by using the result in Figure 1. The experimental cation shifts obtained in Chapter II and the cation-water oxygen distances used were presented in Table III in this chapter. The cation-oxygen distances are the values from the X-ray diffraction studies.[10-13] The theoretical and experimental shifts are compared in Table III. Table III indicates that the theoretical shifts are larger than the experimental ones.

In a study of this type, we should be satisfied with a qualitative agreement with the available experimental data. There are at least three probable sources of error. First, a point-charge model is too crude an approximation to cation-water association. We should include atomic orbitals of the ion. Second, there are errors due to use of the 4-31G basis set (without gauge factors) in the magnetic calculations. Although the 4-31G magnetic shielding values are considerably more accurate than those calculated by using a minimal set,[14] it does not allow an estimate of the Hartree-Fock limit value of σ_H.[15] However, gauge dependences of σ_H will be canceled in the calculation of the shielding change, Δ_C. Finally, there are errors due to the counterion effect and the dielectric constant of the solvent. This calculation neglected the fields originating from counterions and dipolar solvent molecules. Usually, we assume the dielectric constant in vacuum, ε_0, for the space intervening between the point charge and the water molecule. This is not necessarily correct, but the vacuum value is reasonably considered to be much better than the bulk value of acetone, $20.7\varepsilon_0$, in this case by reason of the dielectric saturation effect.[16] The shielding effect of the anions and the polarization of the acetone solvent would attenuate the electrostatic field of the cations and make the calculated Δ_C smaller.

Among the above three sources of error, we suppose that the dielectric effect is the most important. The effect of a dielectric constant should be discussed briefly. Buckingham[17] showed that the σ^d effect depends on the relative dielectric constant, ε_r, inversely, but the σ^p term is proportional to ε_r^{-2}. The σ^d term is much larger than the σ^p term on cation hydration. Therefore, we can simply assume that the total σ change by ion, namely, Δ_C, depends on ε_r inversely. I calculated the appropriate ε_r value from the observed Δ_C's of alkali and alkaline earth metal ions and obtained 1.35 as the effective value for ε_r in acetone solvent. The calculated Δ_C values for ε_r=1.35 are shown in Figure 2 with the results for ε_r=1.

TABLE III. Experimental Polarization Shifts, Δ_C, of Alkali and Alkaline Earth Perchlorates in Acetone and Metal Ion-Oxygen Distances, r.

Salt	Δ_C(obs)[a] (ppm)	r (nm)	Δ_C(calc)[b] (ppm)
$LiClO_4$	1.87	0.21[c]	2.03
$NaClO_4$	0.90	0.24[d]	1.64
$Mg(ClO_4)_2$	3.36	0.204[e]	4.06
$Ca(ClO_4)_2$	2.31	0.243[e]	3.04
$Sr(ClO_4)_2$	1.71	0.26[f]	2.69
$Ba(ClO_4)_2$	1.47	0.29[f]	2.22

[a]Difference between the coordinated and free water proton chemical shifts, i.e., $\Delta_C(obs)=\delta(coordinated)-\delta(free)$.

[b]The vacuum value for the dielectric constant is assumed.

[c]Ref. 10.

[d]Ref. 11.

[e]Ref. 12.

[f]Ref. 13.

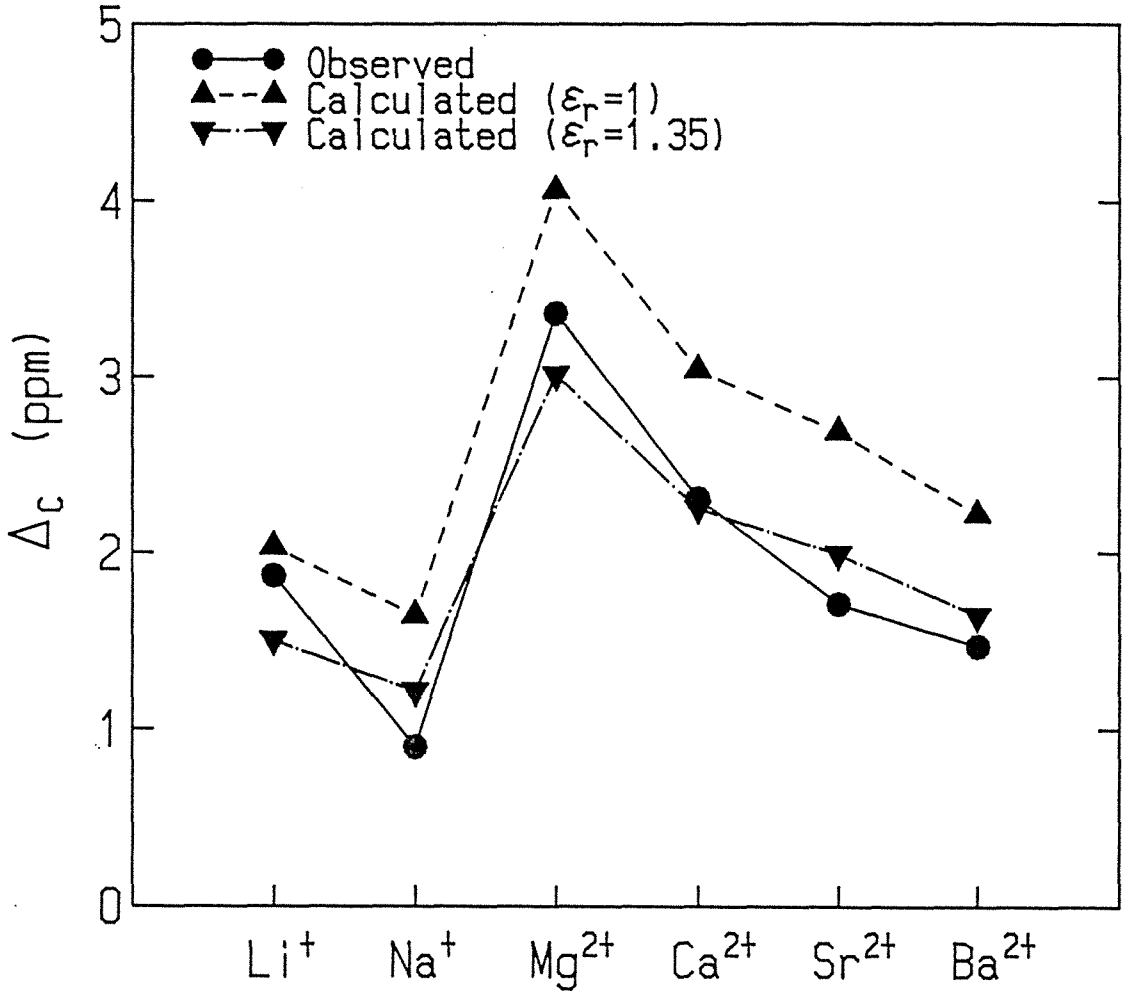

Figure 2. Graphic display of the observed and calculated Δ_C depending on the cation. ε_r is the relative dielectric constant assumed in the calculation.

(B) *Anion-Water Interaction Proton Shift*

I have calculated the shielding constants of the water proton due to a negative point charge. Calculated results are shown in Table IV and Figure 3. The negative charge was set on the hydrogen-oxygen bond axis as drawn in Figure 3, on the basis of the X-ray diffraction study.[9]

Figure 3 shows that the calculated shielding constants decrease with the decreasing distance r. In the calculation of shielding due to a negative point charge, the paramagnetic effect is large compared with the case of positive charge. In this case σ^p contribution represents approximately 35% of the total change.

Table V shows the experimental proton shielding changes, Δ_C(obs), the anion-water proton distances obtained from X-ray diffraction,[9] and the theoretical complex formation shifts, Δ_C(calc). Table V indicates that the experimental Δ_C values are very small compared with the theoretical ones. This result corresponds well with the expectation that the water-acetone hydrogen bonding will obstruct water-anion associations as stated in this introduction. Therefore, it is reasonably concluded that an anion can form only a very weak complex with water in acetone solvent.

TABLE IV. Calculated Magnetic Shielding Constants of Proton in H_2O with the Distance r between Hydrogen and Univalent Negative Point Charge.

r (nm)	σ^d (ppm)	σ^p (ppm)	σ (ppm)	Δ_C(calc) (ppm)
0.15	20.142	0.175	20.318	5.60
0.20	21.366	0.772	22.139	3.78
0.30	22.540	1.407	23.947	1.97
0.40	23.040	1.682	24.722	1.20
0.60	23.445	1.900	25.349	0.57
1.00	23.676	2.022	25.698	0.22
without charge	23.820	2.097	25.917	0.00

TABLE V. Experimental Polarization Shifts, Δ_C, of Tetra-*n*-butylammonium Salts in Acetone and Halide Ion-Proton Distances, r.

Salt	Δ_C(obs) (ppm)	r (nm)	Δ_C(calc)[a] (ppm)
$(n\text{-Bu})_4Cl$	0.75	0.224[b]	3.21
$(n\text{-Bu})_4Br$	0.47	0.244[b]	2.81
$(n\text{-Bu})_4I$	0.06	0.274[b]	2.32
$(n\text{-Bu})_4ClO_4$	0.03	0.294[c]	2.04

[a]The vacuum value for the dielectric constant is assumed.

[b]Ref. 9.

[c]Estimated from the ionic radius of ClO_4^-.

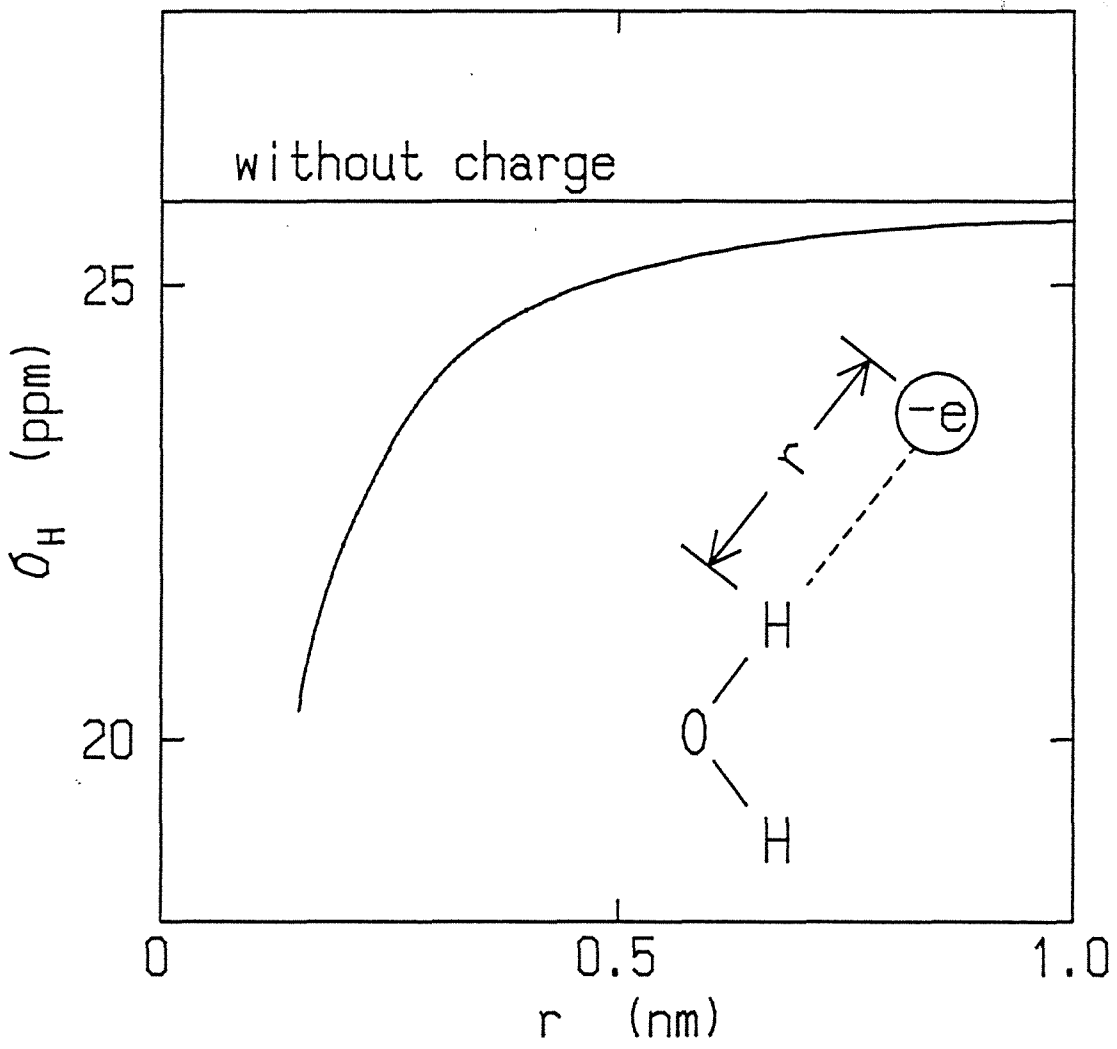

Figure 3. Variation of the calculated proton shielding constant in H_2O with the proton-negative point charge separation, r.

(C) *^{17}O Chemical Shift*

The shielding constants of the water oxygen due to a point charge were also calculated. The calculated ^{17}O shieldings are shown in Table VI-VIII. Figures 4 and 5 represent shielding changes owing to positive and negative point charges, respectively. Figures 4 and 5 indicate that the calculated shielding constants of the water oxygen show an increase, contrary to the case of proton, with the decreasing distance between a point charge and a water molecule. However, since any experimental results for ^{17}O chemical shift variation due to ion hydration have not been reported yet, we cannot confirm the high field shift of the oxygen absorption, which is expected from this calculation. Furthermore, Tables VI-VIII show that in the variation of ^{17}O shifts due to ion hydration, the paramagnetic contribution is overwhelmingly larger than the diamagnetic one. This result means that the oxygen shielding change in ion hydration is predominated by the paramagnetic effect.

TABLE VI. Calculated Magnetic Shielding Constants of Oxygen 17 in H_2O with the Distance r between Oxygen and Univalent Positive Point Charge.

r (nm)	σ^d (ppm)	σ^p (ppm)	σ (ppm)
0.15	416.13	-52.94	363.19
0.20	415.88	-65.41	350.47
0.30	415.69	-80.95	334.74
0.40	415.60	-88.05	327.56
0.60	415.54	-93.83	321.71
1.00	415.50	-97.07	318.43
without charge	415.47	-99.00	316.47

TABLE VII. Calculated Magnetic Shielding Constants of Oxygen 17 in H_2O with the Distance r between Oxygen and Divalent Positive Point Charge.

r (nm)	σ^d (ppm)	σ^p (ppm)	σ (ppm)
0.15	416.54	-38.56	377.98
0.20	416.16	-44.93	371.23
0.25	415.99	-56.80	359.19
0.30	415.87	-66.30	349.57
0.40	415.72	-78.34	337.38
0.60	415.59	-88.93	326.66
1.00	415.52	-95.18	320.34
without charge	415.47	-99.00	316.47

TABLE VIII. Calculated Magnetic Shielding Constants of Oxygen 17 in H_2O with the Distance r between Hydrogen and Univalent Negative Point Charge.

r (nm)	σ^d (ppm)	σ^p (ppm)	σ (ppm)
0.15	415.78	-79.40	336.39
0.20	415.68	-83.26	332.42
0.30	415.59	-89.63	325.96
0.40	415.54	-93.10	322.44
0.60	415.51	-96.12	319.39
1.00	415.49	-97.89	317.59
without charge	415.47	-99.00	316.47

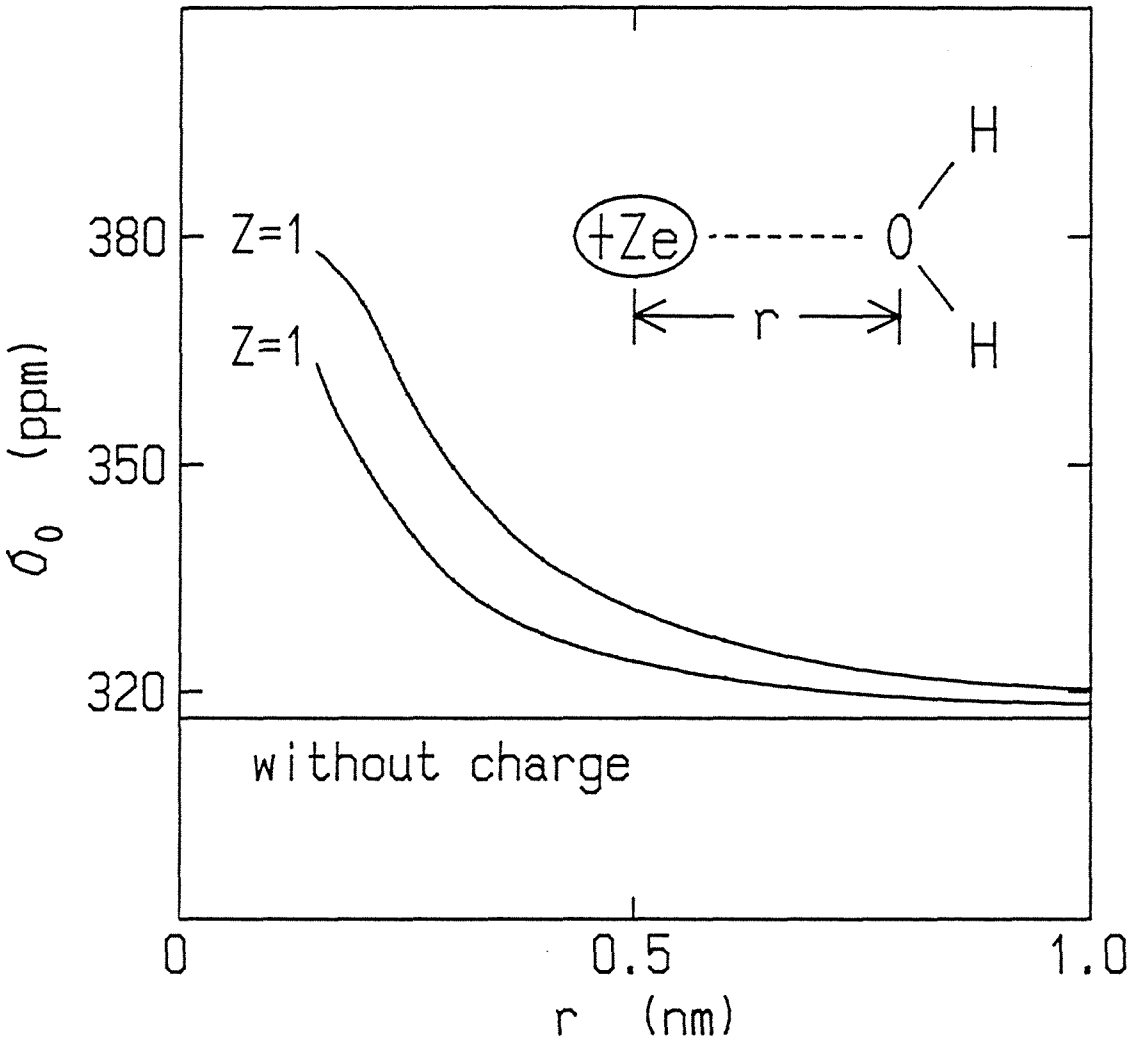

Figure 4. Variation of the calculated oxygen 17 shielding constant in H_2O with the oxygen-positive point charge separation, r.

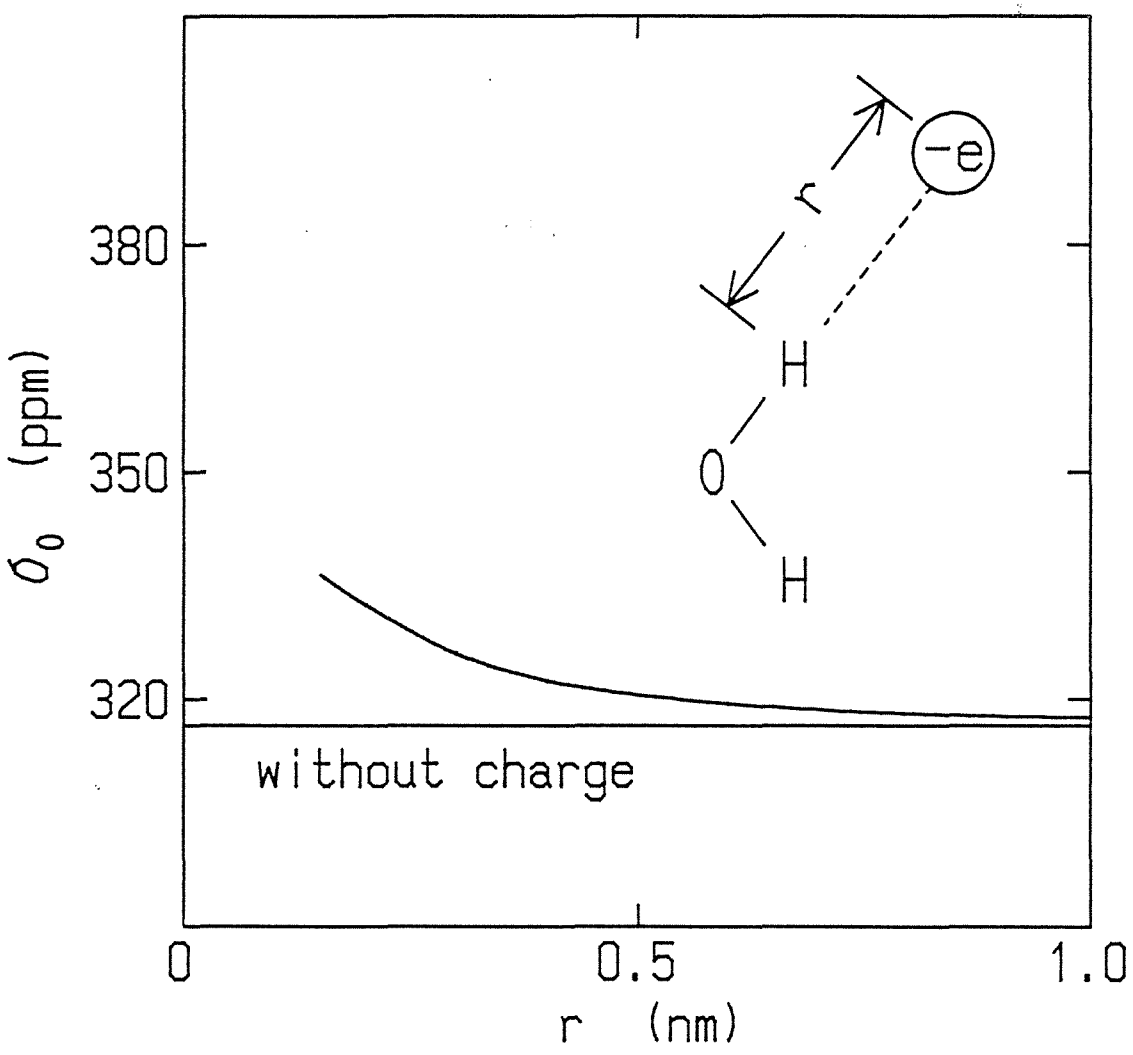

Figure 5. Variation of the calculated oxygen 17 shielding constant in H_2O with the proton-negative point charge separation, r.

References

(1) J. F. Hinton and E. S. Amis, *Chem. Rev.*, 67, 367 (1967).

(2) J. N. Shoolery and B. J. Alder, *J. Chem. Phys.*, 23, 805 (1955).

(3) N. F. Ramsey, *Phys. Rev.*, 78, 699 (1950).

(4) B. Day and A. D. Buckingham, *Mol. Phys.*, 32, 343 (1976).

(5) J. P. Riley and W. T. Raynes, *Mol. Phys.*, 32, 569 (1976).

(6) A. J. Sadlej and W. T. Raynes, *Mol. Phys.*, 35, 101 (1978).

(7) R. Ditchfield, W. J. Hehre, and J. A. Pople, *J. Chem. Phys.*, 54, 724 (1971).

(8) K. Dressler and D. A. Ramsey, *Phil. Trans. Roy. Soc. London*, A251, 553 (1959).

(9) R. M. Lawrence and R. F. Kruh, *J. Chem. Phys.*, 47, 4758 (1967).

(10) T. Radnai, G. Pálinkás, Gy. I. Szász, and K. Heinzinger, *Z. Naturforsch.*, 36a, 1076 (1981).

(11) M. Maeda and H. Ohtaki, *Bull. Chem. Soc. Jpn.*, 48, 3755 (1975).

(12) R. Caminiti, G. Licheri, G. Piccaluga, and G. Pinna, *Chem. Phys. Lett.*, 47, 275 (1977).

(13) G. Palinkas, W. O. Riede, and K. Heinzinger, *Z. Naturforsch.*, 32a, 1137 (1977).

(14) R. Ditchfield, *J. Chem. Phys.*, 65, 3123 (1976).

(15) P. Lazzeretti and R. Zanasi, *J. Chem. Phys.*, 68, 1523 (1978).

(16) W. A. Millen and D. W. Watts, *J. Am. Chem. Soc.*, 89, 6051 (1967).

(17) A. D. Buckingham, *Can. J. Chem.*, 38, 300 (1960).

Chapter IV

Chloride Ion-Trihalomethane Interaction

1 Introduction

Behavior and local structure of electrolytes in solution have an importance in solution chemistry. In the previous chapters, I reported the studies on the ^{1}H chemical shifts with regard to interaction between ion and water molecule.

A remarkable development of multinuclear pulse FT NMR apparatus in recent years has fairly facilitated observations of nuclei with low detectable sensitivity, such as ^{35}Cl. The stable isotope chlorine, i.e., ^{35}Cl, has the electric quadrupole moment. Relaxation of quadrupolar nucleus is generally much simpler to interpret than relaxation of nonquadrupolar nucleus. The relaxation of the former is in most cases totally dominated by the quadrupole relaxation, which is normally induced by purely intramolecular interactions modulated by the molecular motion and is proportional to the product of the square of the quadrupolar coupling constant and the correlation time for molecular reorientation. The line width of NMR spectrum is determined by the spin-spin relaxation time. It is well known that the line width of ^{35}Cl NMR spectrum depends largely on the electrostatic environment of the

chlorine nucleus. For example, in dilute aqueous solutions, the ClO_4^- ion is highly symmetric, and the electric field gradient at the Cl nucleus is nearly zero. Really, the ^{35}Cl line width in 0.5 M $Mg(ClO_4)_2$ aqueous solution is less than 5 Hz and determined by the magnetic field inhomogeneity. On the other hand, in the case of CCl_4 molecule, the distribution of surrounding electrons of the Cl atom is unsymmetrical, so that a large electric field gradient is generated and the line width of the ^{35}Cl reaches to 14.5 kHz. Furthermore, the rotational correlation time is proportional to the size of the molecular species, which is also influential to the ^{35}Cl line width.

The line width and the relaxation time of ^{35}Cl NMR provide us much information, i.e., molecular reorientation, size of molecular species, and character of association, and so they have been used by many investigators. For example, we have works on ion binding to biological molecules,[1-4] complex formations between ions and ligand molecules,[5] contact ion pairing,[6-12] ion solvation,[13,14] and rotational motion of molecules.[15] However, no investigations have been reported yet regarding the variation of ^{35}Cl NMR line width on which the chloride ion associates with a molecule through hydrogen bond in solution. In the present work, I have therefore measured the ^{35}Cl line widths in addition to the ^{1}H chemical shifts

for the weakly formed complexes between Cl^- ion, made of tetra-*n*-butylammonium chloride, and trihalomethanes due to the hydrogen bonding reaction in some organic solvents, and I have also investigated solvent dependence for the line widths of the complexed Cl^- ion and the proton chemical shifts of the complexed trihalomethanes.

2 Experiment

Materials. SIGMA reagent grade tetra-*n*-butylammonium chloride was dried by heating it at 70 °C under vacuum for 3 days. The removal of water was confirmed by ^1H NMR.

Special grade chloroform was used as received. Reagent grade bromoform containing *ca.* 11~13 vol% ethanol as a stabilizer was purified as follows. The ethanol in bromoform was removed by repeating three times the process, standing the solvent over activated molecular sieves (5A) for one day and then filtering it.[16] The removal of ethanol was checked by ^1H NMR.

Special grade acetonitrile and carbon tetrachloride were used without further purification. Special grade acetone was twice distilled over freshly dehydrated 4A molecular sieves. Special grade N,N-dimethylformamide (DMF) was dehydrated by storing it over 4A molecular sieves for one day.

Preparation of Samples for NMR Study. The samples

used for the measurements of ^{1}H NMR chemical shifts of trihalomethanes were prepared as follows. The 0.1 M chloroform and bromoform solutions with varying $(n\text{-}C_4H_9)_4NCl$ concentrations over the range 0 to *ca.* 1 M were made up. TMS was used as an internal reference for the proton chemical shift. Similarly, as the samples for the ^{35}Cl NMR measurements, the 0.1 M $(n\text{-}C_4H_9)_4NCl$ solutions containing various haloform concentrations ranging from 0 to 2 M were prepared. The used solvents are acetonitrile, acetone, N,N-dimethylformamide, and carbon tetrachloride.

NMR Measurements. ^{1}H and ^{35}Cl NMR spectra were obtained on a JEOL FX-200 Fourier-transform spectrometer. The ^{1}H and ^{35}Cl resonance frequencies of the instrument are 199.56 MHz and 19.55 MHz, respectively. The observed frequency width of ^{1}H spectrum was 2 kHz and 90° pulse width was 17.5 μs. The accuracy of the measured proton chemical shifts is within ±0.005 ppm. The ^{35}Cl NMR spectral parameters were as follows. Either one of two spectral widths, 2 kHz and 4 kHz, was used depending on the line width of the spectrum. 90° pulse width was 64 μs, repetition time was from 0.13 to 0.6 s, and the number of pulse repetition was between 10,000 and 500,000. A weighting function for FID was not applied to avoid the artificial broadening of the line width. The line width of ^{35}Cl spectrum was measured at the half-height of the

absorption peak. The error in the observed line widths is within ±0.5 Hz. All the ^{1}H and ^{35}Cl NMR measurements were performed by using 10 mm diameter tubes at the room temperature (22.2±0.2 °C).

Viscosity Measurements. The viscosity coefficients of the pure solvents were measured by using an Ostwald viscosimeter at 22 °C.

3 Analysis

^{1}H Chemical Shift. It is known that trihalomethanes (CHF_3, $CHCl_3$, $CHBr_3$, and CHI_3) associate with chloride ion, made of tetraalkylammonium chloride, through hydrogen bond in some organic solvents (CCl_4 and CH_3CN).[17] Assuming 1:1 complex formation between a Cl^- ion and a trihalomethane molecule, the equilibrium of the reaction is

$$CX_3H + Cl^- \rightleftarrows CX_3H\cdots Cl^- \qquad (1)$$

$$K = \frac{[CX_3H\cdots Cl^-]}{[CX_3H][Cl^-]} \qquad (2)$$

where X represents a halogen atom. The trihalomethane proton complexed with Cl^- ion is deshielded compared with the free trihalomethane proton. At ordinary temperature, exchange between the free and complexed forms is so fast that ^{1}H NMR spectrum gives a single peak for the trihalomethane proton at the mean position of two resonance

frequencies corresponding to the free and complexed forms. Therefore, the observed chemical shift δ is given by the equation

$$\delta = \frac{[CX_3H]}{[CX_3H]_0}\delta_F + \frac{[CX_3H\cdots Cl^-]}{[CX_3H]_0}\delta_C \qquad (3)$$

where $[CX_3H]_0$ is the initial concentration of the used trihalomethane (0.1 M in this experiment), and δ_F and δ_C are the characteristic chemical shifts in the free and complexed situations, respectively. The δ_F value was obtained directly from the measurement for the solution without Cl^- ion, but I determined the δ_C and the equilibrium constant K by minimizing the sum of squares of differences between measured shifts and calculated shifts at various Cl^- concentrations.[18]

^{35}Cl NMR Line Width. In the case of the line width of Cl^-, like in the proton chemical shift, the average width $\Delta\nu$, being determined by the small width of the free chloride ion, $\Delta\nu_F$, and the large width of the complexed ion, $\Delta\nu_C$, is observed. The measured line width is given by

$$\Delta\nu = \frac{[Cl^-]}{[Cl^-]_0}\Delta\nu_F + \frac{[CX_3H\cdots Cl^-]}{[Cl^-]_0}\Delta\nu_C \qquad (4)$$

The $\Delta\nu_F$ value was measured directly, but the $\Delta\nu_C$ and K were determined by analyzing the observed line width data in the similar manner to that in the chemical shift.

The mechanism pictured here for the chemical shift and

the line width is undoubtedly over-simplified, nevertheless, it really provides us a useful working scheme, which is in good agreement with the experimental facts available.

4 Results and Discussion

(A) *Proton Shifts of Hydrogen Bonded Trihalomethanes*

The proton chemical shifts of $CHCl_3$ and $CHBr_3$ in the various solutions were obtained as a function of $(n\text{-Bu})_4NCl$ concentration for the fixed haloform concentration. I measured the ^1H chemical shifts using four kinds of solvents, i.e., acetonitrile, acetone, DMF, and CCl_4. Figure 1 shows the variations of chloroform proton shifts in each solvent. Similarly, Figure 2 presents the variation of bromoform proton shifts. In Figures 1 and 2, the marks represent the observed shifts and the solid curves are the computer simulated ones. I assumed in the analysis that $(n\text{-}C_4H_9)_4N^+$ ion is inert and does not form a contact ion pair with Cl^- ion. Agreement between the measured and calculated shieldings was so good that the assumption of 1:1 association between haloform molecule and Cl^- ion is reasonable in the concentration range of this experiment. The free proton shifts δ_F, the complex proton shifts δ_C, and the equilibrium constants K for chloroform in the used solvents are listed in Table I. Table II likewise shows the results for bromoform. Both Tables I and II show an

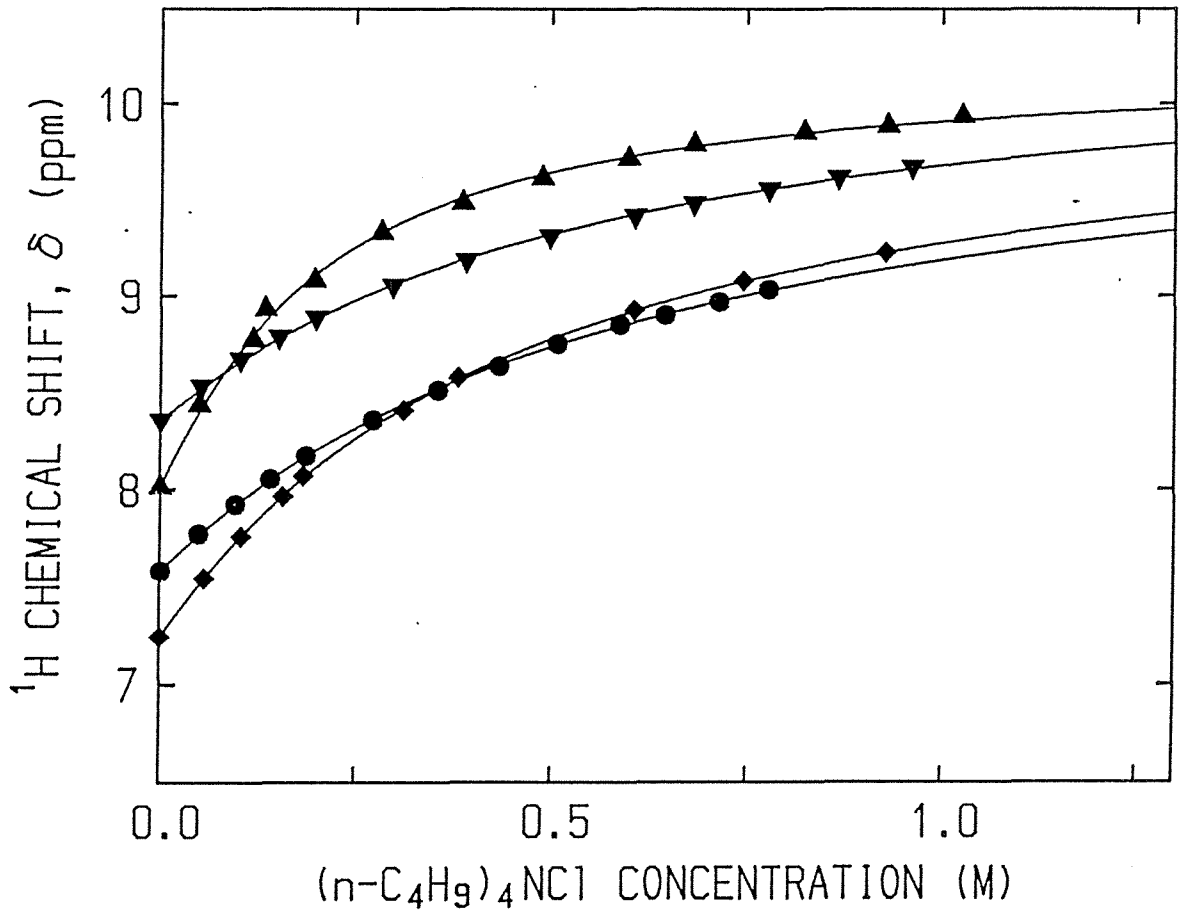

Figure 1. Proton chemical shift of 0.1 M chloroform as a function of $(n\text{-}C_4H_9)_4NCl$ concentration in four solvents, acetonitrile (●), acetone (▲), DMF (▼), and CCl_4 (◆). The solid lines indicate the simulated curves.

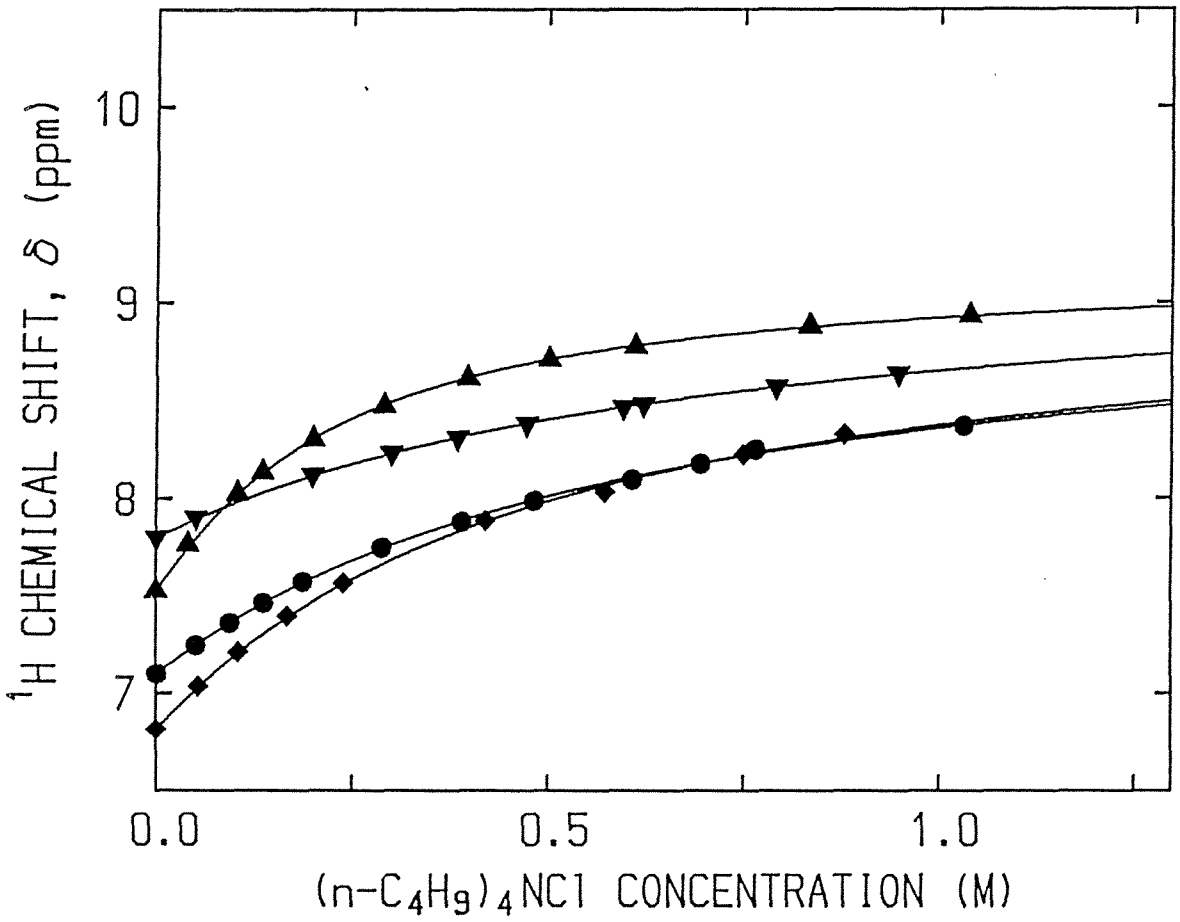

Figure 2. Proton chemical shift of 0.1 M bromoform as a function of $(n\text{-}C_4H_9)_4NCl$ concentration in four solvents, acetonitrile (●), acetone (▲), DMF (▼), and CCl_4 (◆). The solid lines indicate the simulated curves.

TABLE I. Free and Complexed Chloroform Proton Shifts and Equilibrium Constants of Chloroform-Cl^- Ion Association, at 22.2 °C.

Solvent	δ_F (ppm)	δ_C (ppm)	K (M^{-1})
CCl_4	7.24	10.13±0.08	2.55±0.16
CH_3CN	7.58	10.12±0.11	1.84±0.15
$(CH_3)_2CO$	8.01	10.22±0.03	6.61±0.41
DMF	8.36	10.37±0.06	2.05±0.14

TABLE II. Free and Complexed Bromoform Proton Shifts and Equilibrium Constants of Bromoform-Cl^- Ion Association, at 22.2 °C.

Solvent	δ_F (ppm)	δ_C (ppm)	K (M^{-1})
CCl_4	6.81	9.06±0.08	2.44±0.21
CH_3CN	7.10	9.05±0.07	1.95±0.14
$(CH_3)_2CO$	7.52	9.18±0.02	5.93±0.26
DMF	7.80	9.19±0.06	1.68±0.16

interesting result that the free shifts δ_F for chloroform and bromoform depend upon the solvents, but the complexed shifts δ_C for $CHCl_3$ and $CHBr_3$ are almost independent of the solvents and nearly constant.

The free proton shift δ_F is determined by the interaction between a trihalomethane molecule and a solvent one. A large electronegativity of halogen atom lowers the electron density of the hydrogen atom in the trihalomethane, and thus this hydrogen wears the property as an electron acceptor. Therefore, the trihalomethane molecule will form a weak hydrogen bond with a solvent molecule if it has the electron donor property, and then the trihalomethane proton NMR in the electron donor solvent has a peak at a lower magnetic field than that in an inert solvent. The donor number (DN) is known as one of the parameters indicating the extent of the electron donor character.[19] The donor numbers of the used solvents except CCl_4 are shown in Table III. The free proton shifts δ_F of $CHCl_3$ and $CHBr_3$ in DMF, which has the largest donor number, were the highest in the used solvents. One may conclude that the free haloform proton shift δ_F is considerably dependent on the electron donor property of solvent. Furthermore, Tables I and II show that the δ_F value of chloroform in every solvent is about 0.5 ppm larger than that of bromoform. Since the electronegativities of Cl and Br are

3.0 and 2.8, respectively,[20] the hydrogen atom in chloroform is more electrophilic than that in bromoform. Therefore, the chloroform proton presents the lower δ_F value than the bromoform proton does for the same solvent.

I will next discuss the complexed shifts δ_C. Considering the structure of the complexed trihalomethane, it is difficult to assume that the complexed trihalomethane hydrogen and a solvent molecule directly associate. Accordingly, the value of δ_C is independent of solvent and is determined by the hydrogen bond strength between haloform molecule and Cl^- ion.

Furthermore, Tables I and II indicate that the equilibrium constants K in acetone are 2 to 3 times larger than those in the other solvents. I will consider this problem in the following subsection.

TABLE III. Donor Numbers (DN) of the Solvents.

Solvent	DN[a]
CH_3CN	14.1
$(CH_3)_2CO$	17.0
DMF	26.6

[a] Ref. 19.

(B) *^{35}Cl Line Widths of Hydrogen Bonded Cl^- Ion*

The line widths of ^{35}Cl NMR spectra of Cl^- ion were measured as a function of trihalomethane concentration for the fixed Cl^- concentration, using three kinds of solvents, acetonitrile, acetone, and DMF. Chloroform and bromoform were used as trihalomethanes. As an example, Figure 3 shows the variation of ^{35}Cl NMR spectra of Cl^- ion in DMF solvent containing 0.1 M $(n\text{-Bu})_4NCl$ and various concentrations of chloroform. Figures 4 and 5 present the changes of line width of Cl^- ion as a function of trihalomethane concentration, i.e., the chloroform and bromoform concentrations, respectively. The marks, like in the case of proton chemical shifts, mean the measured line widths at half height of the observed peaks, and the solid curves represent the simulated ones obtained with the best fitted parameters. The line widths of free chloride ion $\Delta\nu_F$, the line widths of complexed Cl^- ion $\Delta\nu_C$, and the equilibrium constants K for chloroform in the used solvents are listed in Table IV. The results for bromoform are listed in Table V.

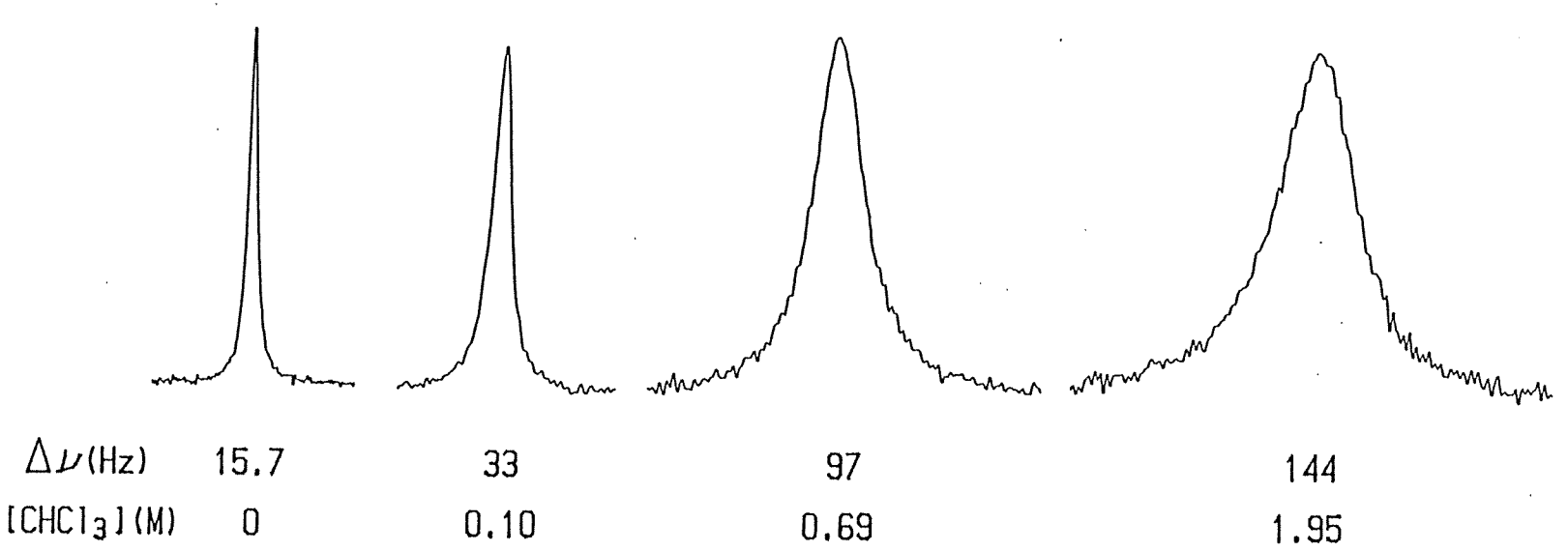

Figure 3. ^{35}Cl NMR spectra of Cl^- ion, made of 0.1 M $(n\text{-Bu})_4NCl$, at various chloroform concentrations in DMF.

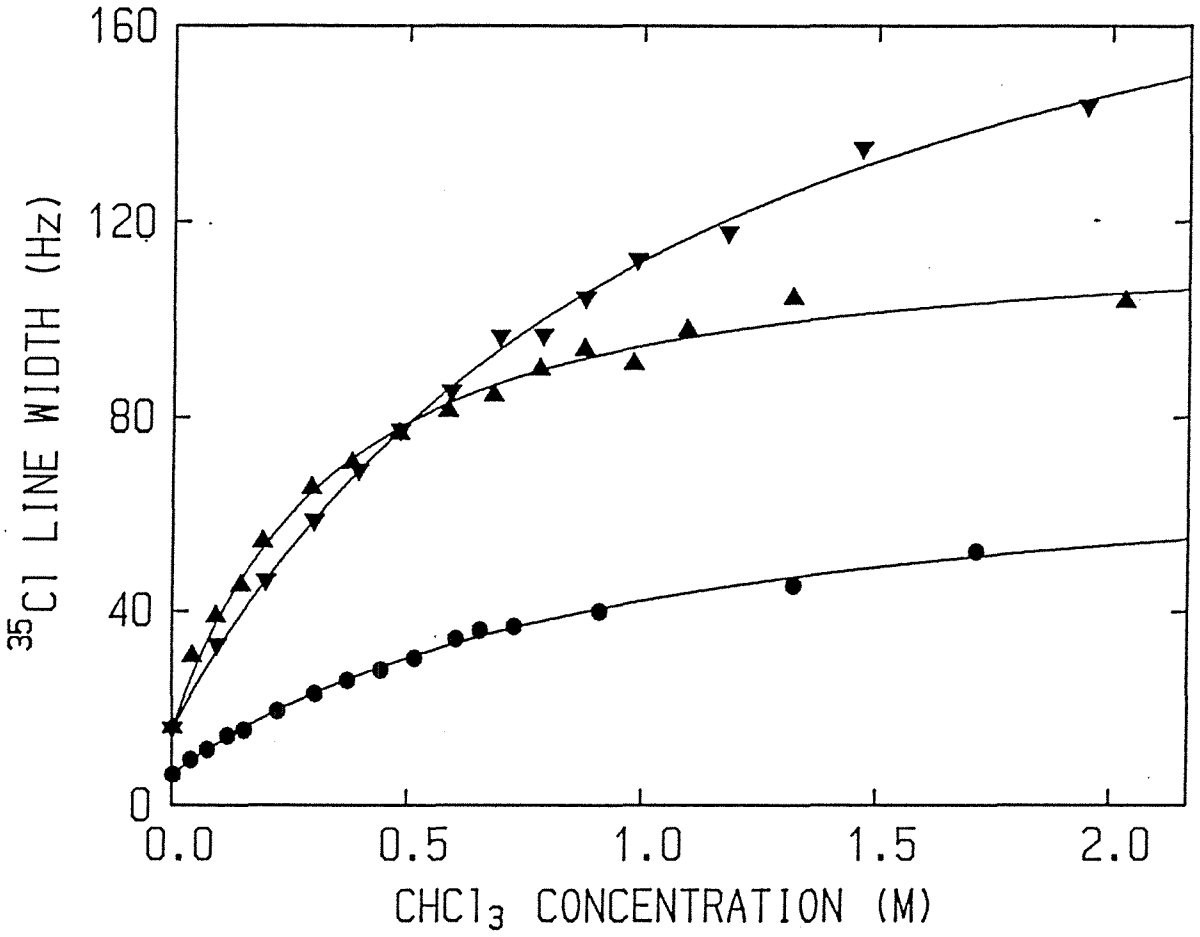

Figure 4. ^{35}Cl line width of Cl^- ion, made of 0.1 M $(n\text{-}Bu)_4NCl$, as a function of chloroform concentration in three solvents, acetonitrile (●), acetone (▲), and DMF (▼).

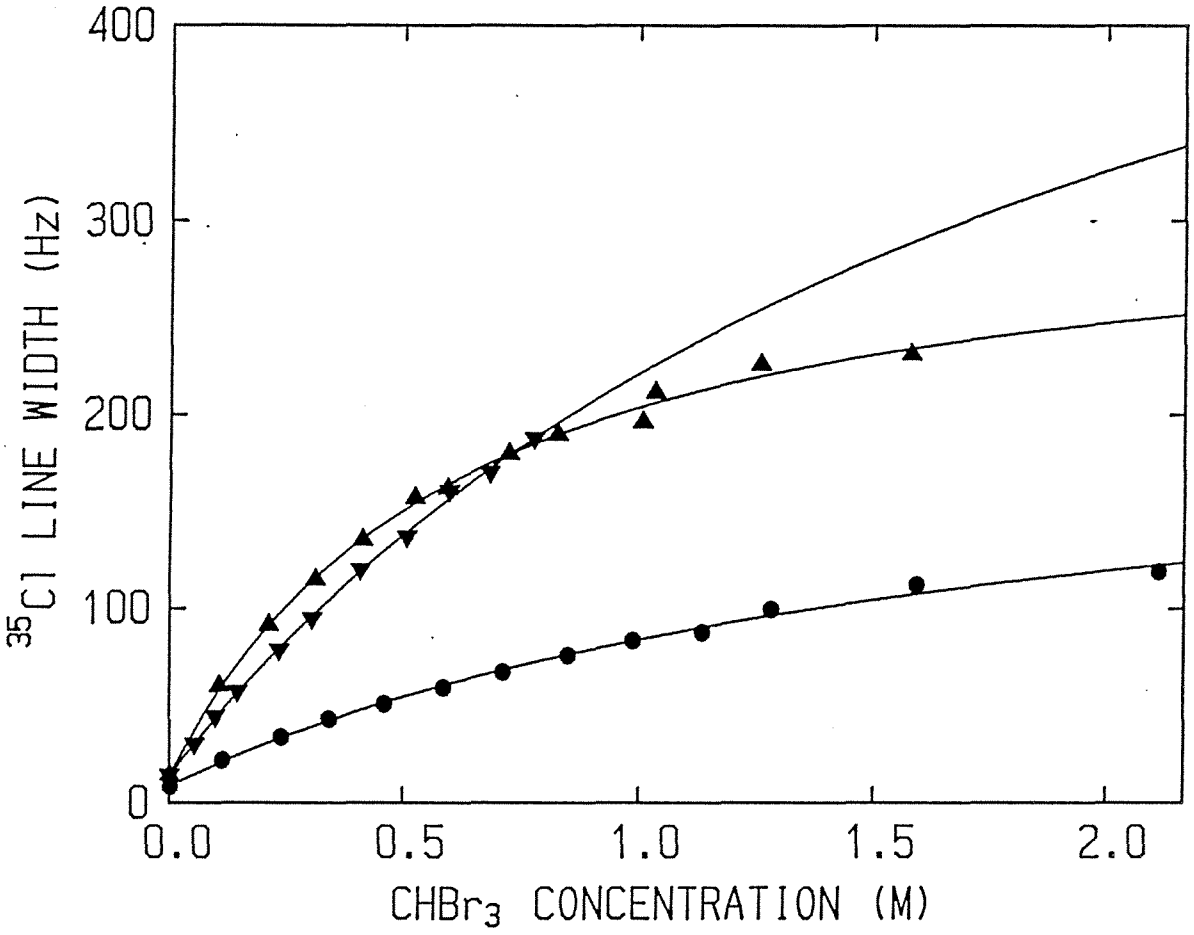

Figure 5. ^{35}Cl line width of Cl^- ion, made of 0.1 M $(n\text{-}Bu)_4NCl$, as a function of bromoform concentration in three solvents, acetonitrile (●), acetone (▲), and DMF (▼).

TABLE IV. ^{35}Cl NMR Line Widths for Free and Complexed Chloride Ions in Chloroform-Cl^- Ion System and Equilibrium Constants of Chloroform-Cl^- Ion Association, at 22.2 °C.

Solvent	$\Delta\nu_F$ (Hz)	$\Delta\nu_C$ (Hz)	K (M^{-1})
CH_3CN	6.2	75±3	1.12±0.08
$(CH_3)_2CO$	15.6	118±2	3.63±0.29
DMF	15.7	214±7	0.99±0.06

TABLE V. ^{35}Cl NMR Line Widths for Free and Complexed Chloride Ions in Bromoform-Cl^- Ion System and Equilibrium Constants of Bromoform-Cl^- Ion Association, at 22.2 °C.

Solvent	$\Delta\nu_F$ (Hz)	$\Delta\nu_C$ (Hz)	K (M^{-1})
CH_3CN	8.1	215±12	0.59±0.06
$(CH_3)_2CO$	13.5	313± 8	1.85±0.13
DMF	14.0	634±71	0.52±0.08

Tables IV and V show that the $\Delta\nu_C$ depends on the solvents in contrast to the case of δ_C. Generally, the line width of a nucleus having a quadrupole moment is controlled by the quadrupolar relaxation. The extreme narrowing condition applies to the liquid state, and the NMR line width at half height $\Delta\nu$ is given by[21]

$$\Delta\nu = \frac{1}{\pi T_2} = \frac{3\pi}{10h^2} \frac{2I+3}{I^2(2I-1)} \left(1+\frac{a^2}{3}\right)(e^2Qq)^2\tau_C \qquad (5)$$

where T_2 is the spin-spin relaxation time, I is the nuclear spin quantum number, a is the asymmetry parameter, Q is the quadrupole moment, q is the electric field gradient at the nucleus, and τ_C is the correlation time for molecular reorientation. In eq 5 e^2Qq is specifically called the quadrupole coupling constant. If it is assumed that the environment of the chlorine nucleus has a cylindrical symmetry, the asymmetry parameter a is zero. Then eq 5 for chlorine nucleus of spin I=3/2 reduces to

$$\Delta\nu = \frac{2\pi}{5h^2} (e^2Qq)^2\tau_C \qquad (6)$$

Equation 6 means that the line width is simply proportional to square of the quadrupole coupling constant times correlation time, and so the line width of the complexed Cl^- ion depends on the two factors, one of which is the electric field gradient eq at the chlorine nucleus and the other the

correlation time τ_C of the complexed chloride ion. I attempted to remove the effect of τ_C from the complexed line width $\Delta\nu_C$. In order to simplify the treatment, I assumed that τ_C is proportional to the viscosity of the pure solvent, η.[6] This leads to the assumption that $\Delta\nu_C/\eta$ is independent of τ_C. The measured η's and the $\Delta\nu_C/\eta$'s are listed in Table VI, which shows that the $\Delta\nu_C/\eta$ values for acetonitrile and DMF solvents are similar to each other, but that the $\Delta\nu_C/\eta$'s are larger for acetone than for the other solvents. This trend is analogous to that for the equilibrium constant.

TABLE VI. Viscosity Coefficient η, Relative Dielectric Constant $\varepsilon/\varepsilon_0$ (ε and ε_0 are the dielectric constants of solvent and in vacuum, respectively), and Line Width of Complexed Cl^- Ion Divided by the Viscosity of Solvent, $\Delta\nu_C/\eta$.

Solvent	η (cP)	$\Delta\nu_C/\eta$ (Hz/cP)		$\varepsilon/\varepsilon_0$ [a]
		$CHCl_3$	$CHBr_3$	
CH_3CN	0.364	207	591	36.0
$(CH_3)_2CO$	0.326	362	960	20.7
DMF	0.893	240	710	36.7

[a] Ref. 19.

We consider here the electric field gradient, eq. When the chloride ion forms a hydrogen bond with a trihalomethane molecule, the electronic structure of the system can be described as a resonance between two structures, Cl^- H-CX_3 and Cl-H CX_3^-. Therefore, we may describe the total electronic wave function of Cl^-, Ψ, as a linear combination of the nonbonding Cl^- ion wave function, Ψ_I, and the covalently bonded Cl-H wave function, Ψ_{II}, according to the valence bond method. Then we have

$$\Psi = \Psi_I + C\Psi_{II} \qquad (7)$$

where C will depend on the covalent character between the Cl^- ion and the haloform hydrogen. Ψ_{II} differs from Ψ_I in the point that the lone pair electrons of Cl^- in Ψ_I are changed to the covalent bond electrons between the Cl atom and the haloform hydrogen in Ψ_{II}. If the coordinate origin is put at the nuclear position of the Cl^- and the electrostatic potential produced by the electrons at the point x′,y′,z′ is expressed by V(x′,y′,z′), the electric field gradient at the origin, eq, is given by

$$eq = \left(\frac{\partial^2 V}{\partial z'^2}\right)_{x'=y'=z'=0} = \frac{Ce}{\sqrt{2}\pi\varepsilon_0} \langle \chi_{Cl} | \frac{r^2-3z^2}{r^5} | \chi_H \rangle \qquad (8)$$

where r is the distance of an electron from the chlorine nucleus and z represents the z coordinate of the electron.

The binding axis between haloform and Cl^- is taken as the z axis. ε_0 is the dielectric constant in vacuum. We used, in the derivation of eq 8, the fact that Ψ_I is the wave function of the spherical Cl^- ion and does not produce any field gradient. In eq 8, χ_{Cl} is the sp^3 hybrid orbital of Cl^- and χ_H is the hydrogen 1s orbital. In Table VI, the relative dielectric constants of the solvents, $\varepsilon/\varepsilon_0$,[19] are listed. It is experimentally found that $\Delta\nu_C/\eta$ relates with $\varepsilon/\varepsilon_0$. We may assume that the covalent character, i.e., the coefficient C would be smaller in the solvent having a larger dielectric constant.

Tables IV and V further show that the $\Delta\nu_C$ of the Cl^--bromoform complex are about three times as large as compared with those of the chloroform complex. The difference in the ^{35}Cl line widths between the chloroform and bromoform complexes should be explained. The rotational correlation time τ_C is proportional not only to the viscosity η but also to the volume of the complex v, as given in the equation

$$\tau_C = v\eta/kT \qquad (9)$$

Since the volume of Cl^--bromoform complex is larger than that of Cl^--chloroform complex, the ^{35}Cl line width of the bromoform complex is larger than that of the chloroform complex in the same solvent. Furthermore, it seems that the electron cloud of trihalomethane molecule contributes to

the electric field gradient at the chlorine nucleus. This effect may also lead to the larger ^{35}Cl line width of the bromoform complex because of the larger electron cloud in the bromoform molecule. However, at present we cannot separate these two contributions.

We now consider about the equilibrium constants K obtained from the Cl^- line widths, which are listed in Tables IV and V. The equilibrium constants in acetonitrile and DMF are nearly equal, but the K's in acetone are three times as large as compared with those in the other solvents. This trend resembles the result of K obtained from the haloform proton shifts. However, each of the K values evaluated from the line widths is smaller than the K from the proton shifts, and the former is of one third to one half of the latter. The equilibrium constant K is related to the free energy difference ΔG^0 between two states, the complexed state and the free state. Namely,

$$\Delta G^0 = -RT\ell nK \qquad (10)$$

Evidently, ΔG^0 will be proportional to the electrostatic potential V produced by the Cl^- ion, which in turn is inversely proportional to the dielectric constant ε. We can expect that acetone whose $\varepsilon/\varepsilon_0$ is smaller than those of the other solvents should give a larger K value as compared with acetonitrile and DMF. This expectation is consistent

with the experimentally found equilibrium constants, which were independently determined from two kinds of quantities, the proton chemical shifts and the ^{35}Cl line widths.

Finally, the difference between the equilibrium constant acquired from the chemical shifts and that from the line widths has to be discussed. Essentially the equilibrium constant K should be defined with the activities of the individual species. To calculate the equilibrium constant correctly, we have to use the different activity coefficients in two different experimental conditions, i.e., the case of the ^{1}H chemical shift measurements where the Cl^- concentration was varied for the fixed low haloform concentration and the case of the line width measurements where the haloform concentration was varied for the fixed low Cl^- concentration. However, I neglected variation of the activity coefficients in my analysis. This neglect may be the cause of the difference between the K's obtained from the chemical shifts and the line widths.

References

(1) T. R. Stengle and J. D. Baldeschwieler, *Proc. Natl. Acad. Sci. (U.S.A.)*, 55, 1020 (1966).

(2) A. C. Plaush and R. R. Sharp, *J. Am. Chem. Soc.*, 98, 7973 (1976).

(3) B. Jönsson and B. Lindman, *FEBS Lett.*, 78, 67 (1977).

(4) J. A. Happe and R. L. Ward, *J. Phys. Chem.*, 83, 3457 (1979).

(5) T. Sugawara, M. Yudasaka, Y. Yokoyama, T. Fujiyama, and H. Iwamura, *J. Phys. Chem.*, 86, 2705 (1982).

(6) H. A. Berman and T. R. Stengle, *J. Phys. Chem.*, 79, 1001 (1975).

(7) M. S. Greenberg and A. I. Popov, *J. Solution Chem.*, 5, 653 (1976).

(8) P. Reimarsson and B. Lindman, *Inorg. Nucl. Chem. Lett.*, 13, 449 (1977).

(9) M. Yudasaka, T. Sugawara, H. Iwamura, and T. Fujiyama, *Bull. Chem. Soc. Jpn.*, 54, 1933 (1981).

(10) A. G. Miller, J. A. Franz, and J. W. Macklin, *J. Phys. Chem.*, 89, 1190 (1985).

(11) J. Ogino, H. Suezawa, and M. Hirota, *Chem. Lett.*, 889 (1983).

(12) H. Suezawa, T. Kodama, J. Ogino, and M. Hirota, *Chem. Lett.*, 1645 (1984).

(13) D. C. McCain, *J. Inorg. Nucl. Chem.*, 42, 1185 (1980).

(14) M. Yudasaka, T. Sugawara, H. Iwamura, and T. Fujiyama, *Bull. Chem. Soc. Jpn.*, 55, 311 (1982).

(15) W. Storek, *Chem. Phys. Lett.*, 98, 267 (1983).

(16) R. D. Green and J. S. Martin, *J. Am. Chem. Soc.*, 90, 3659 (1968).

(17) S. Shimokawa, H. Fukui, J. Sohma, and K. Hotta, *J. Am. Chem. Soc.*, 95, 1777 (1973).

(18) D. R. Burfield, *J. Chem. Educ.*, 56, 486 (1979).

(19) U. Mayer, *Stud. Phys. Theor. Chem.*, 27, 219 (1982).

(20) L. Pauling, *The Nature of the Chemical Bond*, 3rd ed., (Cornell University Press, New York, 1960).

(21) J. A. Pople, W. G. Schneider, and H. J. Bernstein, *High Resolution Nuclear Magnetic Resonance*, (McGraw-Hill, New York, 1959).

Chapter V

Anisotropic Rotational Motion of Water Molecule Bound to Al^{3+} Ion

1 Introduction

In Chapter II, I reported changes of the water proton chemical shifts due to ion hydration. These changes of the chemical shifts provide information on the static properties of ion-water complex formation. In addition to this, however, it is also important to have information concerning the dynamical motion of the water molecules in aqueous salt solutions in order to have a better understanding of ion-water interactions. Up to the present a number of investigations relating to the dynamics of the hydration shell have been performed by the use of NMR techniques.[1] There are three kinds of motions in water molecules, namely, translational, rotational, and vibrational motions. The first two, i.e., translational and rotational motions, are measurable with NMR instruments. The rate of the translational motion of the water molecules in the first coordination sphere can be estimated from the exchange rate between the bound and free waters, which is obtained from line shape analysis,[2,3] line width measurement at half-height of the water signals,[4-6] and the transverse relaxation time, T_2, measured by the pulsed NMR method.[7]

Information on the rotational motion of water molecules can be acquired from measurement of the longitudinal relaxation time, T_1,[8] and that of the ^{17}O signal width.[9]

For many metal ions, it has been found that on the bound water molecules in solutions the rotational diffusion rate about the axis O-M (M = metal ion), $R_{\parallel}$, is more rapid than that of the O-M axis itself, $R_{\perp}$.[10] However, for the Al^{3+} ion Hertz et al.[8] have concluded that these two rotational diffusion rates, $R_{\parallel}$ and $R_{\perp}$, of the water molecules in the first hydration sphere are almost equal to each other in aqueous $AlCl_3$ solutions at room temperature. This conclusion indicating the isotropic rotation of the water molecules bound to the Al^{3+} ion was obtained from the measurement of the ^1H spin-lattice relaxation time, T_1, at 25 °C, at which the observed value of T_1 is the average of the T_1 from the coordinated water and the T_1 from the uncoordinated water. Moreover, at this temperature the measured T_1 contains contributions from both the translational and rotational motions. Therefore, their conclusion regarding the motion of the waters bound to Al^{3+} may include some ambiguity.

It is well-known that when aluminum salt solutions are cooled to low temperatures, the proton NMR signal of water separates into two components corresponding to coordinated and uncoordinated water molecules.[11-19] This phenomenon

comes from the fact that at sufficiently low temperatures the exchange between the coordinated and bulk water molecules is slow enough to permit the observation of the separate absorption signals. With this condition, we have two advantages to investigate the motion of the hydration water. First, the rate of the translational motion is too slow to contribute to the spin-lattice relaxation. Second, we can determine the relaxation times of the bound and bulk waters independently.[20] Consequently, we can expect more exact information concerning the rotational motion to be obtained by measuring T_1's of the separate signals of the free and coordinated waters at low temperatures. The purpose of the present work is to investigate the rotational motion of the water molecules in aqueous $Al(ClO_4)_3$ solutions by measuring T_1 at temperatures lower than +10 °C, at which separate signals of the bound and free waters are available.

2 Experiment

Materials. Water was distilled and passed over cation- and anion-exchange resins.

The $Al(ClO_4)_3 \cdot 6H_2O$ was synthesized and purified as follows: Special grade $AlCl_3 \cdot 6H_2O$ was dissolved in 20% perchloric acid, in which the molar ratio of $HClO_4$ to Al^{3+} was 3.5:1. The solution was concentrated by heating it

until it ceased to generate hydrogen chloride gas. The solvent was then evaporated under reduced pressure and the residual solid was dried under vacuum. The $Al(ClO_4)_3$ formed was recrystallized from ethanol three or four times until the concentration of Fe^{3+} become lower than the lower limit of detection (5 ppm).

I prepared seven different aqueous solutions as samples, which differed from each other in $Al(ClO_4)_3$ concentration. The mole ratios, H_2O/Al, in each sample were 16.1, 19.6, 23.5, 26.1, 31.5, 35.0, and 39.6, respectively. The Al^{3+} concentration was determined by chelatemetric titration with EDTA at 100 °C. The pH of the solutions was ca. 2, which was independent of the aluminum concentrations of the samples.

NMR measurements. The ^1H NMR spectra were obtained on a JEOL FX-200 Fourier-transform spectrometer (199.56 MHz for ^1H) equipped with a JEOL NM-PVTS2 variable-temperature unit. The spin-lattice relaxation times, T_1, were obtained by the inversion-recovery method using the pulse sequence of $(-\ 180°\ \text{pulse} - t - 90°\ \text{pulse} - T\ -)_n$. For each measurement of T_1, more than 15 different pulse intervals (t) were used. The delay time (T) was 10 s because all the absorption signals had T_1 values shorter than 0.5 s. The number of the pulse sequence (n) was 4. The measurements of ^1H NMR were performed by using 5-mm-

diameter tubes at temperatures of +10 to -65 °C. The accuracy in the temperature was within ±0.2 °C.

Prior to the experiment, the effect of the dissolved oxygen in a sample was examined. The T_1 of the undegassed sample was compared with that of the degassed and sealed sample at the same temperature and salt concentration. It was confirmed that the difference between both the T_1's was small and within the experimental error in this temperature range. Therefore, the undegassed samples were used for my experiments.

3 Results and Discussion

T_1 of coordinated and bulk water protons. As described previously, when aqueous solutions including the Al(III) ions were cooled, exchange of water molecules was considerably slowed and separate proton signals were observed for the bulk water and the coordinated water bound to Al^{3+}. This phenomenon is illustrated in Figure 1. The ratio of the separate peak areas of B_{H_2O} and C_{H_2O} in Figure 1 indicated that the hydration number of Al^{3+} was about six. This hydration number is the same as that in the results of Fratiello et al.[15] Therefore, the peak of C_{H_2O} in Figure 1 arises from the water molecules in the first hydration sphere.

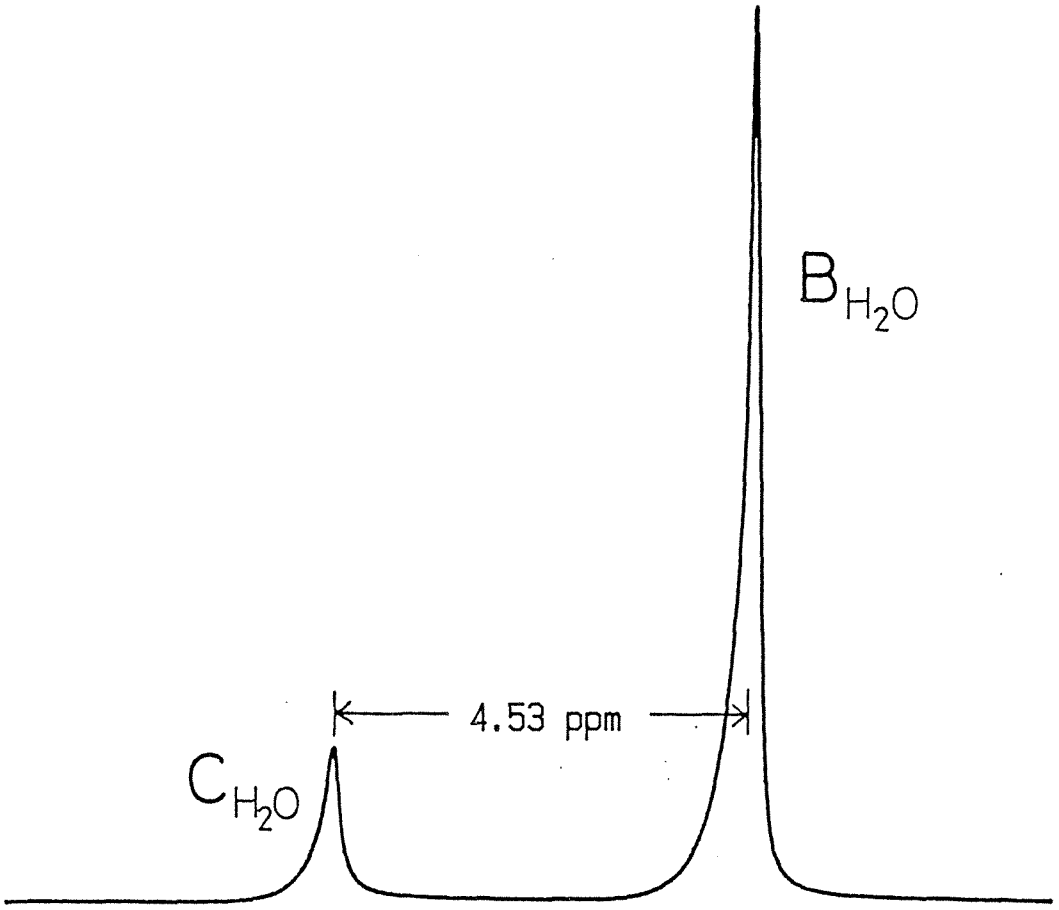

Figure 1. The proton magnetic resonance spectrum of the aqueous $Al(ClO_4)_3$ solution at -40.9 °C. The mole ratio between H_2O and Al is 31.5:1. The signals arising from bulk water (B_{H_2O}) and the water molecules in the Al^{3+} hydration shell (C_{H_2O}) are labeled.

I measured the spin-lattice relaxation times, T_1, of the coordinated and free water molecules as a function of temperature for the seven samples with different $Al(ClO_4)_3$ concentrations. All inversion-recovery measurements of T_1 showed a single exponential form throughout the temperature range. This means that the exchange rate between the coordinated and bulk water molecules is negligibly small at the temperatures at which the coordinated and uncoordinated water signals have different T_1 values.[20,21] The results for the two solutions with high and low aluminum concentrations in the samples measured are shown in Figure 2. Figure 2 indicates that the T_1 values of the coordinated and bulk water protons are equal at relatively high temperatures, but the difference between the two T_1's arises as the temperature falls below ca. -20 °C. The other five measured solutions showed a similar trend. The differences between the T_1 values of the coordinated and uncoordinated water molecules were especially large at low temperatures and low aluminum concentrations. The difference between the bulk and coordinated T_1's seems to reflect the dynamics of the water molecules in the hydration shell of the aluminum ion. I will attempt below to explain the experimental results by assuming anisotropic rotational motion of the coordinated water. Figure 2 shows that at low salt concentrations the minimum of T_1(coordinated) is

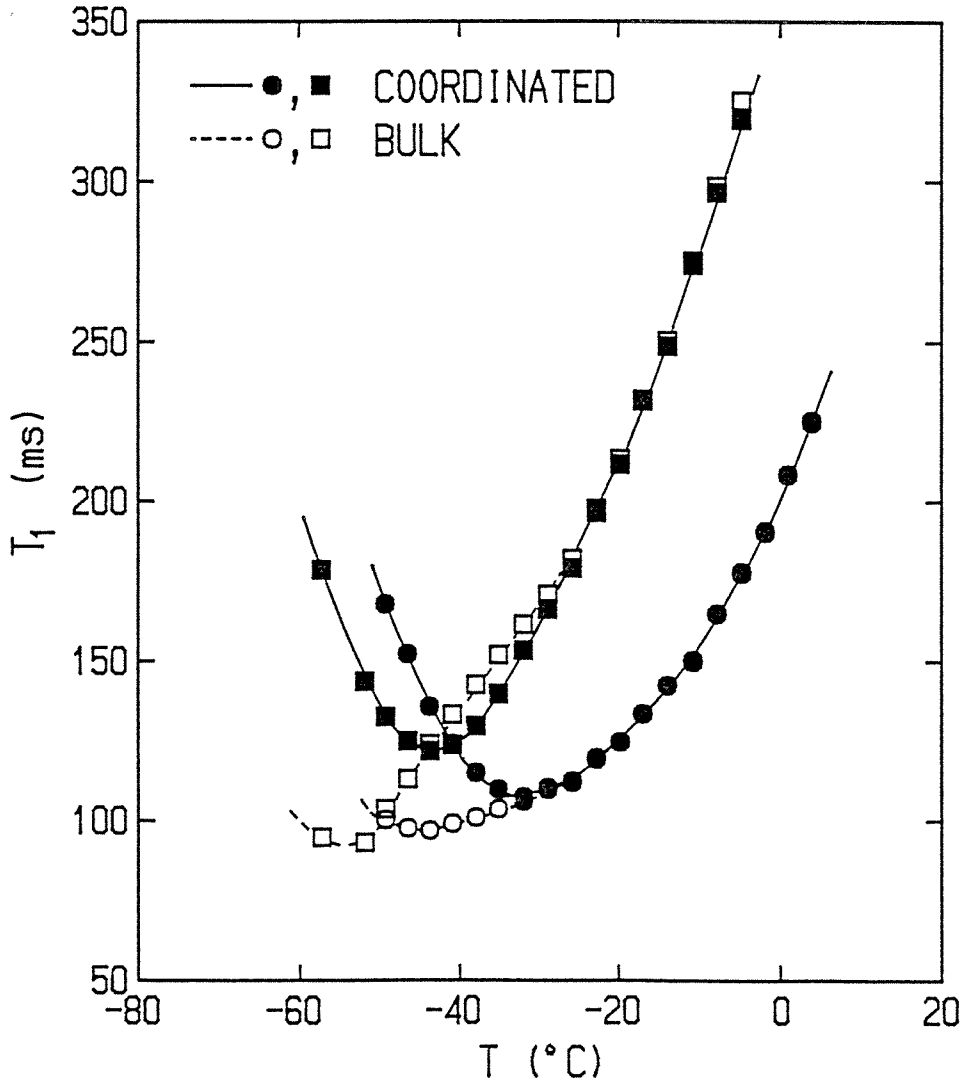

Figure 2. The ^1H spin-lattice relaxation times, T_1, of the coordinated and bulk water signals as a function of temperature, T, at high (o and •) and low (□ and ■) aluminum concentrations. The mole ratios of H_2O to Al is 19.6 (o and •) and 31.5 (□ and ■), respectively.

longer than that of T_1(bulk). Moreover, $[T_1(\text{coordinated})]_{min}$ is at higher temperature than $[T_1(\text{bulk})]_{min}$. These experimental facts can be explained by assuming the anisotropic motion of the coordinated water molecule.

Anisotropic rotational motion of the coordinated waters. It is reasonable to assume that the velocity of translational motion is comparable to the exchange rate between the coordinate and bulk water molecules. We can expect that the measured relaxation rates, $1/T_1$, in this experiment will not contain a contribution of the translational motion in either the bound or the free waters, because the spin-lattice relaxation time depends on rapid motions as fast as the Larmor precession and the velocity of translational motion is estimated to be less than 10^3 s^{-1}. Therefore, we have to explain the experimental results by the rotational motion contribution to T_1. Moreover, the correct explanation should be able to account for the experimental fact that the two T_1's of the coordinated and uncoordinated water signals are equal at high temperatures, but they differ from each other at low temperatures.

The intermolecular protons are more separated from each other in comparison with the two intramolecular protons. The rotational relaxation rate is inversely proportional to the sixth power of the dipole-dipole distance, and so the rotational intermolecular interactions in the clusters such

as $(H_2O)_n$ and $Al(H_2O)_6^{3+}$ can be safely neglected.[8] Furthermore, the contributions from the proton-cation (Al^{3+}) and the proton-anion (ClO_4^-) magnetic dipole -dipole interactions are also negligible by the same reason. As a consequence of these simplifications, we can use the single molecule approximation for either the bound or the free waters. I postulated that only the intramolecular proton-proton interaction operating within a single H_2O molecule undergoing the rotational motion contributes to the measured relaxation rates of the water protons for either the bound or the free waters.

I needed three more assumptions in order to interpret the difference between the T_1's of the coordinated and bulk water protons. These three assumptions are as follows:

(i) Bulk water molecules rotate isotropically. Namely, the motion of bulk molecules is described by a spherically symmetric rotation in which the Brownian motion is represented by the single rotational diffusion coefficient, R. On the other hand, coordinated water molecules rotate anisotropically as an axially symmetric ellipsoidal body does. Namely, the motion of coordinated molecules is described by the axially symmetric rotation in which the Brownian motion is represented by the two rotational diffusion coefficients, i.e., the rotational diffusion coefficient about the symmetric axis, $R_{\parallel}$, and that

about the two equivalent axes perpendicular to the symmetric axis, $R_\perp$. I introduced the anisotropy parameter, σ, which is defined as the ratio of $R_\perp$ to $R_\parallel$. That is,

$$\sigma = R_\perp / R_\parallel \qquad (1)$$

(ii) The three rotational diffusion coefficients, R, $R_\parallel$, and $R_\perp$, are functions of the temperature and the aluminum concentration of the solution.

(iii) The angle between the symmetric axis of rotation for the coordinated water molecule and the proton-proton vector in this molecule is fixed to be 90°. This is shown in Figure 3. We took a model in which the symmetric axis of rotation, i.e., C_2 axis of the coordinated water, coincides with the binding axis in the complex formation between the Al^{3+} ion and the water oxygen.

Under the above three assumptions, I analyzed the rotational motions of the coordinated and bulk water molecules. For this aim I utilized the formulae of T_1 by Woessner[22,23] and Shimizu[24] for an ellipsoidal body.

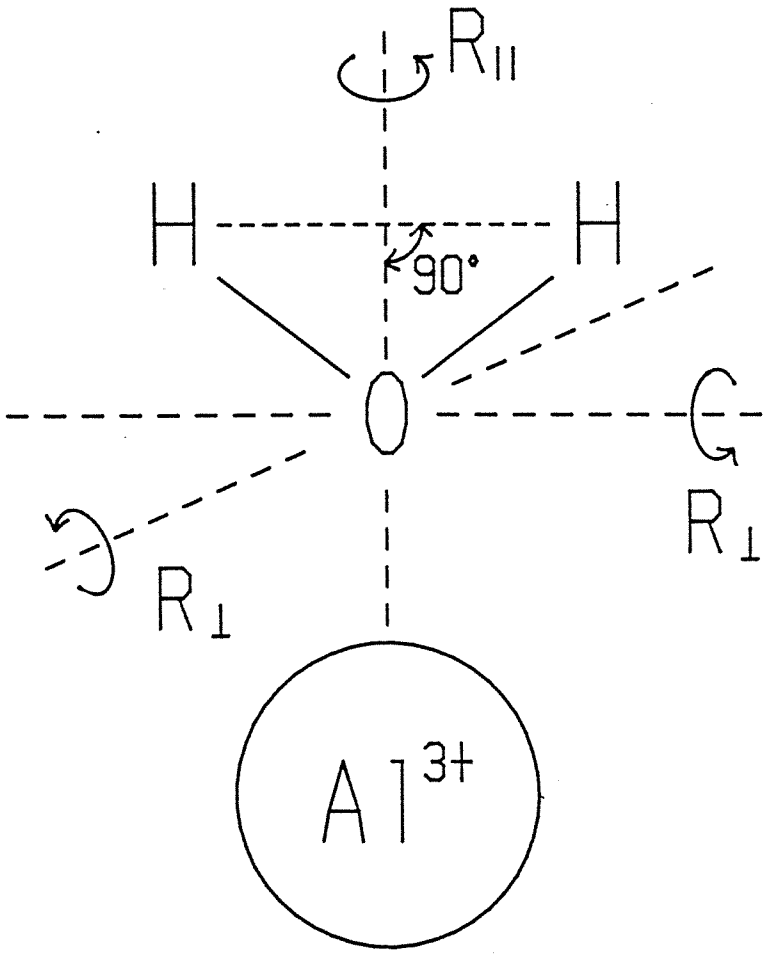

Figure 3. The model used for the motion of the water molecules coordinated to the Al^{3+} ion.

Woessner[23] has shown that the nuclear spin-lattice relaxation time, T_1(aniso), for two interactive protons fixed in a molecule undergoing axially symmetric anisotropic rotation is given by

$$\frac{1}{T_1(\text{aniso})} = \frac{3}{10}\left(\frac{\mu_0}{4\pi}\right)^2 \frac{\gamma_H^4 \hbar^2}{r_{HH}^6 \omega_H}[f(x,\sigma)+2f(2x,\sigma)] \qquad (2)$$

where

$$f(x,\sigma) = \frac{1}{4}\frac{6\sigma x}{x^2+(6\sigma)^2} + \frac{3}{4}\frac{(4+2\sigma)x}{x^2+(4+2\sigma)^2} \qquad (3)$$

$$x = \omega_H / R_{11} \qquad (4)$$

In eq 2 μ_0 is the magnetic permeability in vacuo, γ_H is the magnetogyric ratio of proton, r_{HH} is the proton-proton distance in the water molecule, and ω_H is the Larmor angular frequency of the proton. In this experiment, $\omega_H = 4\times10^8\pi\ s^{-1}$. The above formulae for T_1(aniso) become the same as the well-known T_1(iso) formula in the isotropic rotational motion if σ is set equal to unity. That is,

$$\frac{1}{T_1(\text{iso})} = \frac{3}{10}\left(\frac{\mu_0}{4\pi}\right)^2 \frac{\gamma_H^4 \hbar^2}{r_{HH}^6 \omega_H}\left[\frac{6y}{y^2+36} + \frac{24y}{4y^2+36}\right] \qquad (5)$$

where $y=\omega_H/R$, and $1/R=6\tau_C$, with the usual correlation time τ_C.

Figure 2 indicates that the minimum value of T_1(bulk) is about 95 ms, which is in good agreement with the theoretical $[T_1(\text{bulk})]_{min}$ of 102 ms, calculated from eq 5 with the H-H distance of ice (r_{HH}=0.1645 nm, r_{OH}=0.101 nm, ∠HOH=109°).

Equations 2 and 5 indicate that the ratio, $[T_1(\text{aniso})]_{min}/[T_1(\text{iso})]_{min}$, is the function of the anisotropy parameter σ alone. It is easily shown that

$$1 \leq [T_1(\text{aniso})]_{min}/[T_1(\text{iso})]_{min} \leq 4/3 \qquad (6)$$

None of my results were contradictory with eq 6. In fact, the ratios, $[T_1(\text{coordinated})]_{min}/[T_1(\text{bulk})]_{min}$, for all samples measured were within the above limitation. We now realize that all the three parameters of R, $R_{\parallel}$, and $R_{\perp}$ can be determined at the particular temperature of $[T_1(\text{coordinated})]_{min}$. I was able to evaluate these parameters at that temperature by the following three steps. First, σ i.e., $R_{\perp}/R_{\parallel}$ was determined by comparing the experimental ratio, $[T_1(\text{coordinated})]_{min}/[T_1(\text{bulk})]_{min}$, with the theoretical ratios, $[f(y,1)+2f(2y,1)]_{max}/[f(x,\sigma)+2f(2x,\sigma)]_{max}$, calculated for various values of σ. Next, for a given σ, $R_{\parallel}$ was estimated from the particular value of x giving the maximum for the function,

$[f(x,\sigma)+2f(2x,\sigma)]$. Finally, I obtained R at the temperature of $[T_1(\text{coordinated})]_{min}$ by comparing the experimental ratio, $T_1(\text{bulk})/[T_1(\text{bulk})]_{min}$, with the theoretical ratio, $1.4252/[f(y,1)+2f(2y,1)]$, in which $1.4252=[f(y,1)+2f(2y,1)]_{max}$. The three parameters, R, $R_{\parallel}$, and $R_{\perp}/R_{\parallel}(=\sigma)$, at the particular temperature of $[T_1(\text{coordinated})]_{min}$ are plotted against the mole fraction of $Al(ClO_4)_3$, X_{Al}, in Figure 4.

Figure 4 shows that the rotational velocity of the bulk water, R, monotonously decreases with increasing salt concentration, but $R_{\parallel}$ of the coordinated water has a maximum at the mole fraction of ca. 0.04. Moreover, $R_{\perp}$ of the hydration water is abruptly slowed as the mole fraction of Al decreases. The concentration dependence of the bulk water motion R is the same as that usually observed for rotational diffusion. This is easily accounted for by the higher microviscosity for bulk water at higher concentrations. However, the coordinated water motion shows quite a different dependence on the concentration. The behavior of $R_{\parallel}$ implies the presence of two opposed sources of resistance for the motion, one of which is the microviscosity effect and gives for $R_{\parallel}$ the same dependence on the concentration as R, but the other source of resistance makes $R_{\parallel}$ slower for lower concentrations.

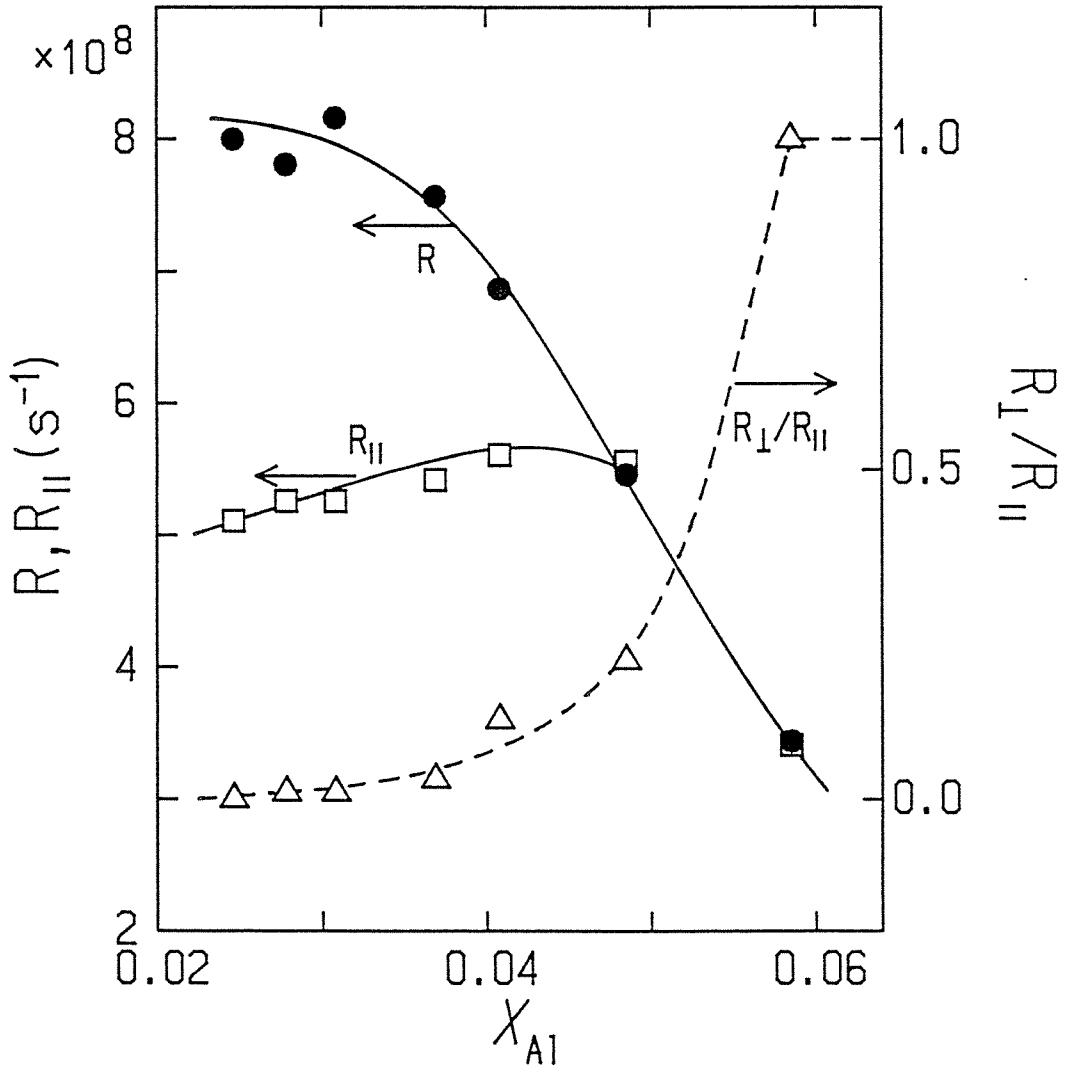

Figure 4. The three rotational diffusion coefficients, R (●) $R_{\perp}$ (□), and $R_{\perp}/R_{\perp}(=\sigma)$ (△), at the temperature of $[T_1(\text{coordinated})]_{\text{min}}$ as a function of the mole fraction of $Al(ClO_4)_3$, X_{Al}. The curve for $R_{\perp}$ coincides with the curve for R in the region higher than X_{Al}=0.05.

Furthermore, for $R_\perp$, the latter source, giving slower motion for lower concentrations, is much stronger than the former viscosity contribution providing the same concentration dependence as R. Therefore, the slowdown of $R_\perp$ is more rapid than that of $R_\parallel$ for lowering the concentration of Al. The anisotropy parameter σ, i.e., $R_\perp/R_\parallel$, of the coordinated water molecules abruptly falls from unity (indicating isotropic rotation) to zero (completely anisotropic rotation) when the aluminum concentration is lowered. The higher resistance for motion for low concentrations may be attributed to the Al-H_2O coordination bond formation in the hydration shell provided that the bond strength would be larger for low concentration. Thus, I arrived at the conclusion that the structure of the hydration shell becomes looser as the salt concentration increases. This conclusion is supported by another piece of evidence reported by Hertz et al.[8] that the interaction between neighboring hydrated ions destroys the ordered structure of the hydration sphere. The destruction of the hydration shell will lower the heights of the potential barriers against the rotational motions in the shell. Particularly, the motion of the Al-O axis itself, i.e., $R_\perp$ is much accelerated by this destruction.

My experimental results showed that difference between the two T_1's of the coordinated and bulk water signals

becomes greater at lower temperatures and lower aluminum concentrations. This means that $R_{\perp}/R_{\parallel}$ (also maybe $R_{\parallel}/R$) is smaller at lower temperatures and lower Al concentrations.[25] However, the two T_1's were equal at temperatures higher than -20 °C at any $Al(ClO_4)_3$ concentration. Therefore, the conclusion of Hertz et al. that $R_{\parallel}$ is equal to $R_{\perp}$ will be correct only at the higher temperature.

References

(1) H. G. Hertz, *Water, A Comprehensive Treatise*, edited by F. Franks, (Plenum Press, New York, 1973), Vol. 3, Chapter 7.

(2) D. Fiat and R. E. Connick, *J. Am. Chem. Soc.*, 90, 608 (1968).

(3) R. G. Wawro and T. J. Swift, *J. Am. Chem. Soc.*, 90, 2792 (1968).

(4) T. J. Swift and R. E. Connick, *J. Chem. Phys.*, 37, 307 (1962).

(5) R. E. Connick and D. J. Fiat, *Chem. Phys.*, 44, 4103 (1966).

(6) J. W. Neely and R. E. Connick, *J. Am. Chem. Soc.*, 94, 3419 (1972).

(7) M. Grant and R. B. Jordan, *Inorg. Chem.*, 20, 55 (1981).

(8) H. G. Hertz, R. Tutsch, and H. Versmold, *Ber. Bunsenges. Phys. Chem.*, 75, 1177 (1971).

(9) R. E. Connick and K. Wüthrich, *J. Chem. Phys.*, 51, 4506 (1969).

(10) H. G. Hertz, R. Tutsch, and N. S. Bowman, *J. Phys. Chem.*, 1976, 80, 417 (1976).

(11) R. E. Schuster and A. Fratiello, *J. Chem. Phys.*, 47, 1554 (1967).

(12) A. Fratiello and R. E. Schuster, *Tetrahedron Lett.*, 4641 (1967).

(13) A. Fratiello, R. E. Lee, V. M. Nishida, and R. E. Schuster, *J. Chem. Phys.*, 47, 4951 (1967).

(14) A. Fratiello and R. E. Schuster, *J. Chem. Educ.*, 45, 91 (1968).

(15) A. Fratiello, R. E. Lee, V. M. Nishida, and R. E. Schuster, *J. Chem. Phys.*, 48, 3705 (1968).

(16) N. A. Matwiyoff, P. E. Darley, and W. G. Movius, *Inorg. Chem.*, 7, 2173 (1968).

(17) A. Fratiello, R. E. Lee, V. M. Nishida, and R. E. Schuster, *Inorg. Chem.*, 8, 69 (1969).

(18) G. K. Schweitzer and J. F. Stephens, *Spectrosc. Lett.*, 3, 11 (1970).

(19) A. Fratiello, *Progr. Inorg. Chem.*, 17, 57 (1972).

(20) W. Koch, I. Wawer, and H. G. Hertz, *Z. Phys. Chem. (Frankfurt am Main)*, 132, 161 (1982).

(21) J. B. Lambert and J. W. Keepers, *J. Magn. Reson.*, 38, 233 (1980).

(22) D. E. Woessner, *J. Chem. Phys.*, 36, 1 (1962).

(23) D. E. Woessner, *J. Chem. Phys.*, 37, 647 (1962).

(24) H. Shimizu, *J. Chem. Phys.*, 37, 765 (1962).

(25) At temperatures low enough to satisfy $x,y>>1$, the ratio $T_1(\text{aniso})/T_1(\text{iso})$ is equal to $2(R/R_{II})/(1+\sigma)$.

Chapter VI

Summary and Conclusion

In Chapters II to V the author reported on the static and dynamic information obtained by NMR for the ion -molecule interactions in solution. In the present chapter the author presents the summary and conclusion for the work described in this thesis.

In Chapter II, I reported on the measurements and analysis of the water proton chemical shifts due to the diamagnetic ion-water interactions in acetone solvent. The association constants K and complex formation shifts Δ_C were determined by assuming a one-to-one complex formation between a water molecule and a diamagnetic cation or anion. The results indicated that the complex formation shifts of metal salts are dominated by metal ions and relatively unaffected by anions, whereas the equilibrium constants of association are greatly affected by anions. The relationship between the equilibrium constant and the ionic size and charge was investigated, and the same relationship for the complex shift was also investigated. Clear relationships of K and Δ_C against the ionic size and charge were found for alkali and alkaline earth metal ions. This suggests that the equilibrium constant and the complex shift

of these ions were determined by the electrostatic interaction between the ion and water molecule. However, any relationships were not found for K and Δ_C of anions and cations other than the alkali and alkaline earth metal ions.

In Chapter III, the theoretical calculation for the ion-water association shifts was described. I performed ab initio calculations for the shielding changes of the water proton and oxygen with a point charge model. The calculated proton shielding changes caused by presence of a point charge were compared with the experimental complex shifts for the ion-water associations in acetone, which were shown in Chapter II. Comparing the theoretical shielding changes with the experimental complex shifts, it was concluded that (1) the theoretical calculation leads to a shielding change of 1.6 to 4.1 ppm for the alkali and alkaline earth metal ions, which is in qualitative agreement with the experimental results, and (2) an anion can form only a very weak complex with water in acetone solvent. Furthermore, the effect of the dielectric constant of solution on the complex shifts was discussed.

In Chapter IV, I reported on the chloride ion -trihalomethane interactions. Association due to hydrogen bonding between a chloride ion and a trihalomethane molecule ($CHCl_3$ or $CHBr_3$) in some solvents (carbon tetrachloride, acetonitrile, acetone, and N,N-dimethylformamide) was

studied using ^{1}H NMR chemical shift and ^{35}Cl NMR line width measurements. Analyzing the observed ^{1}H chemical shifts and ^{35}Cl line widths, I obtained the complexed proton shifts of trihalomethanes, the complexed line widths of Cl^- ion, and the equilibrium constants of associations between trihalomethanes and Cl^- ion. The equilibrium constants can be obtained from either the ^{1}H shift or the ^{35}Cl line width. Two kinds of the association constants based on the shift and the line width were compared. The solvent dependence of the complexed Cl^- line widths, of the complexed proton shifts, and of the equilibrium constants were investigated. The complexed shifts of trihalomethanes indicated a constant value regardless of the kinds of solvents. On the other hand, the complexed line widths of Cl^- ion showed an obvious solvent dependence. Furthermore, the equilibrium constants in acetone were three times as large as compared with the values in other solvents.

In Chapter V, I reported on the anisotropic rotational motion of water molecule bound to Al^{3+} ion. The ^{1}H spin -lattice relaxation times, T_1, of the separate free and coordinated water signals of aqueous $Al(ClO_4)_3$ solutions have been independently measured at low temperatures between +10 and -65°C and with varying salt concentrations. All inversion-recovery measurements of T_1 showed a single

exponential form in the above temperature range. It was found that under this low temperature condition, only the intramolecular proton-proton interaction undergoing rotational motion contributes to T_1. The experimental results showed that the difference between the two signals' T_1 values of the free and coordinated waters arises as the temperature falls below ca. -20°C. It was shown that the experimental results could be explained if we assume that the coordinated water molecules would anisotropically rotate as ellipsoidal molecules at low temperatures, whereas the bulk water molecules would isotropically rotate as spherical molecules throughout the temperature range. I applied the theory of spin-lattice relaxation due to the anisotropic rotational diffusion by Woessner to the analysis of the motion of the coordinated water molecules, and obtained the following conclusions: (1) at low temperatures and low aluminum concentrations, the coordinated water molecules undergo anisotropic rotational motion as an axially symmetric ellipsoidal body whose axis of symmetry is the C_2 axis of the H_2O molecule, and (2) the motion of the hydration water molecule is slowed at low Al concentrations.

As a conclusion, it was found that the proton chemical shift provides us an excellent breakthrough to the ion-water interaction problem. The proton shift data are simple and

easily handled. The ^{35}Cl line width measurements offered us consistent results with the ^{1}H chemical shift data. The proton spin-lattice relaxation time of the coordinated water signal was found to be very useful to investigate the motion of the bound water. The oxygen 17 chemical shift would be helpful to inquire into the ion-water interactions if we could find a good reference for ^{17}O signal.

LIST OF PUBLICATIONS RELATED TO THE THESIS

1. Proton Magnetic Resonance Study of Ion Hydration in Acetone
   H. Fukui, K. Miura, T. Ugai, and M. Abe,
   J. Phys. Chem., 81, 1205 (1977).
2. Linear electric field dependence of the proton magnetic shielding
   H. Fukui, Y. Kitamura, and K. Miura,
   Mol. Phys., 34, 593 (1977).
3. Proton Nuclear Magnetic Resonance Study of Ion Hydration in Acetone. 2
   K. Miura and H. Fukui,
   Inorg. Chem., 19, 995 (1980).
4. Calculation of NMR chemical shifts. II.
   Comparison of the SOS and FP methods
   H. Fukui, H. Yoshida, and K. Miura,
   J. Chem. Phys., 74, 6988 (1981).
   Erratum : *Ibid.*, 77, 5259 (1982).
5. Calculation of NMR chemical shifts. IV.
   Hydronium and hydroxyl ions
   H. Fukui, K. Miura, and F. Tada,
   J. Chem. Phys., 79, 6112 (1983).

6. Calculation of NMR chemical shifts. V.
The gauge invariant coupled Hartree-Fock calculation for H_2O, H_3O^+, and OH^-
H. Fukui, K. Miura, H. Yamazaki, and T. Nosaka,
J. Chem. Phys., 82, 1410 (1985).

7. Calculation of NMR chemical shifts. VI.
Gauge invariant and Hermitian condition
H. Fukui, K. Miura, and H. Shinbori,
J. Chem. Phys., 83, 907 (1985).

8. Nuclear Magnetic Resonance Study of Ion Hydration. 3.
Anisotropic Rotational Motion of Water Molecules Bound to the Aluminum (III) Ion
K. Miura, K. Hashimoto, H. Fukui, E. Yamada, and S. Shimokawa,
J. Phys. Chem., 89, 5098 (1985).

9. Calculation of NMR Chemical Shifts. 7.
Gauge Invariant INDO Method
H. Fukui, K. Miura, and A. Hirai,
J. Magn. Reson., 67, 328 (1986).

10. NMR Study on Ion-Molecule Interaction. 4.
^{1}H and ^{35}Cl NMR of Chloride Ion-Trihalomethane Association
K. Miura, M. Tanaka, H. Fukui, and H. Toyama,
J. Phys. Chem., submitted to the editor.

LIST OF PUBLICATIONS NOT DIRECTLY RELATED TO THE THESIS

1. Finite perturbation calculations of the nuclear spin-spin coupling constant for the hydrogen fluoride molecule
   H. Fukui, A. Sanyoshi, and K. Miura,
   J. Chem. Phys., 69, 943 (1978).
2. *Ab initio* calculations of the nuclear spin-spin coupling constants. II. Comparison of the FP and SOS methods
   H. Fukui, K. Miura, and N. Ishigami,
   J. Chem. Phys., 71, 560 (1979).
3. Calculation of the Nuclear Spin-Spin Coupling Constants. 3. σ- and π-Electron Contributions in Some Simple Unsaturated Hydrocarbons
   H. Fukui, T. Tsuji, and K. Miura,
   J. Am. Chem. Soc., 103, 3652 (1981).
4. Calculation of self-consistent-field-Xα wave functions. Core-exchange polarization calculation for free atoms
   H. Fukui, K. Miura, M. Kamitokusari, N. Kobayashi, and J. Sohma,
   Phys. Rev. A, 25, 580 (1982).
5. Calculation of the nuclear spin-spin coupling constants. IV. π-electron contributions
   H. Fukui, K. Miura, K. Ohta, and T. Tsuji,
   J. Chem. Phys., 76, 5169 (1982).

6. Reaction of Rhodium Species with Carbon Monoxide on Freshly Prepared Rh-Y Zeolite and $RhCl_3/SiO_2$ Catalysts Revealed by the ^{13}C NMR Technique

N. Takahashi, K. Miura, and H. Fukui,

J. Phys. Chem., 90, 2797 (1986).

Acknowledgement

The present investigations were carried out from 1976 to 1986 in Department of Industrial Chemistry, Faculty of Engineering, Kitami Institute of Technology.

The author wishes to thank Professor Hiroyuki Fukui, Kitami Institute of Technology, and Professor Junkichi Sohma, Hokkaido University for reading the manuscript and giving him many useful comments. He also expresses his thanks to Professors Kunio Hikichi, Hiroshi Yoshida, and Akihiro Tsutsumi, Hokkaido University, for reviewing of this thesis.

August, 1986

Koichi Miura